American Mineralogist, Volume 80, pages 593–612, 1995

Kinetics of the reaction $H_2O + O = 2OH$ in rhyolitic and albitic glasses: Preliminary results

YOUXUE ZHANG,* E. M. STOLPER, P. D. IHINGER**
Division of Geological and Planetary Sciences, California Institute of Technology, Pasadena, California 91125, U.S.A.

ABSTRACT

The kinetics of homogeneous reactions are important in understanding the cooling history of rocks and in understanding experimental speciation data. We have experimentally studied the kinetics of the interconversion reaction between H_2O molecules and OH groups in natural rhyolitic glasses (0.5–2.3% total water) and a synthetic albitic glass (1% total water) at 400–600 °C. The reaction rate increases with temperature and total water content. Equilibrium is not always approached monotonically; the speciation may first depart from equilibrium and then come back to equilibrium. Experimental reaction rates agree with those inferred from previous speciation data of rhyolitic glasses quenched from 850 °C. The experimental data are modeled successfully by considering both the reaction and the diffusion of OH that brings OH groups together to react. This study shows that species concentrations in glasses quenched from ≤600 °C reflect those at experimental temperatures unless the water content is higher than that used in the present study. Species concentrations in glasses with total water contents ≥0.8 wt% and which were rapidly quenched in water from 850 °C do not represent their equilibrium concentrations in the melt at 850 °C, but record a lower apparent equilibrium temperature that depends on water content and quench rate. Natural rhyolitic glasses and glass inclusions do not record preeruptive melt speciation, though total water content may be conserved. The experimental data are used to infer cooling rates for natural obsidian glasses. Pyroclastic glass fragments from the bb site of Mono Craters have cooling rates similar to air-cooled experimental charges (~3 °C/s). Different types of glasses from the Mono Craters have different cooling rates, which cover four orders of magnitude. Some natural obsidians appear to have had complex cooling histories. The wide range of cooling rates and thermal histories is consistent with previous inferences that some obsidian clasts at the Mono Craters formed as glass selvages lining volcanic conduits or dikes that were subsequently caught up in the explosive eruption, which led to variable degrees of transient heating followed by rapid cooling and deposition. These experimental data reveal surprisingly rich detail in water speciation in volcanic glasses and show how, at least in principle, quantitative constraints on thermal histories can be extracted by experimentation and application of kinetic models.

INTRODUCTION

It is well known that water dissolves in silicate melts as at least two species, OH groups (associated with Al, Si, or other cations) and H_2O molecules. Because the two species play different roles in glass and melt structure and in geological processes, there has been considerable effort to quantify the dependence of the speciation (the concentrations of H_2O and OH) on total water content and temperature (Bartholomew et al., 1980; Bartholomew, 1982; Stolper, 1982a, 1982b, 1989; Newman et al., 1986; Eckert et al., 1989; Silver and Stolper, 1989; Silver et al., 1990; Zhang et al., 1991). These results have been applied to a variety of problems, including (1) the quantitative measurement of water content in natural rhyolitic glasses (e.g., Newman et al., 1988; Dobson et al., 1989; Skirius et al., 1990), (2) the thermodynamics of hydrous components in molten silicates (Silver and Stolper, 1989), (3) the reactions at a molecular scale by which H_2O molecules and the silicate framework interact to produce OH groups (McMillan and Remmele, 1986; Mysen and Virgo, 1986a, 1986b; Eckert et al., 1988, 1989; Kohn et al., 1989a, 1989b; McMillan, 1989; Mysen, 1992; Sykes and Kubicki, 1993), (4) the apparent equilibrium temperatures of natural obsidian glasses (Stolper, 1989), (5) the fractionation of H isotopes between vapor and melt (Taylor, 1986; Newman et al., 1988; Dobson et al., 1989; Ihinger, 1991), and (6) the diffusion of water in rhyolitic glasses and basaltic melts (Zhang et al., 1991; Zhang and Stolper, 1991). Although most applications have been concerned with melt properties at elevated temperature,

* Present address: Department of Geological Sciences, University of Michigan, Ann Arbor, Michigan 48109-1063, U.S.A.
** Present address: Department of Geology and Geophysics, Yale University, New Haven, Connecticut 06511, U.S.A.

003–004X/95/0506–0593$02.00

all quantitative studies of water speciation have thus far been made at room temperature on glasses quenched from higher temperature. In some cases, it has been possible to demonstrate that change in speciation upon quenching is negligible for the reported experimental data (e.g., Stolper, 1989; Zhang et al., 1991). In other cases, and in the absence of quantitative knowledge of how to correct experimental results for the effects of quenching, it has been assumed that the change in speciation known to occur upon quenching is small compared with the effects of other variables such as total dissolved water content and melt composition (e.g., Stolper, 1982b; Silver and Stolper, 1989; Silver et al., 1990). The validity of this assumption and some inferences derived from these glass studies about the dependence of water speciation in melts on total water content and temperature have been challenged by Dingwell and Webb (1990) on the basis of structural relaxation theory.

To test whether previous speciation data and interpretations were compromised by the conversion of OH groups to H_2O molecules during quench, we conducted an experimental study of the kinetics of this process and the reverse process in rhyolitic and albitic glasses. Understanding the kinetics of this reaction may also be useful for inferring aspects of thermal history (e.g., cooling rate and whether cooling was monotonic) from the observed speciation of water in natural volcanic glasses (e.g., Newman et al., 1988). Depending on the reaction rate, the kinetics of the interconversion reaction may also play a role during violent volcanic eruptions because the conversion of OH groups to H_2O molecules often provides the main ingredient for bubble growth. Finally, by studying the kinetics of this reaction, it might be possible to gain insight into aspects of glass structure, such as the dynamics of structural reorganization and the motions of various molecules, cations, and anions in the glass.

Experimental methods

The experiments reported here were all done on glass wafers with known initial H_2O and OH concentrations. (Throughout this paper, "H_2O" refers to molecular H_2O and "total water" refers to the total dissolved water as the sum of dissolved H_2O molecules and OH groups.) Samples were heated and quenched, and species concentrations were then measured using Fourier transform infrared spectroscopy. By repeating this procedure on single specimens, it was possible to examine the variation of species concentrations with duration of heating. In general, experimental procedures follow those of Stolper (1989) and Zhang et al. (1991) and are summarized as follows.

Glass starting materials are rhyolitic obsidians from the Mono Craters in central California with water contents between 0.5 and 2.3% (Table 1) and are described in detail in Newman et al. (1986, 1988) and Zhang et al. (1991). The glass numbers are simplified as A through H, and a key is provided in the footnote of Table 1. The speciation of water in these starting glasses varied for different samples with the same water concentration, presumably due to differences in thermal history. The albitic glass (1% total water) used in this study was synthesized at 1400 °C and 20 kbar in a piston-cylinder apparatus by Silver and Stolper (1989, Sample ABC-26).

Glass fragments were cut into chips and then ground and polished on parallel surfaces to a final thickness of 0.6–3.9 mm prior to the experiment (Table 1). The size and thickness of each glass wafer were chosen according to the experiment conditions: thinner and smaller wafers were used for shorter experiments to minimize the time required for heating to the experimental temperature and for experiments at high water content or high temperature to maximize the quench rate. Thicker and larger samples were used for longer experiments to minimize the effect of the diffusive loss of water. Most doubly polished sections of centimeter size were homogeneous to within 5% of the total water present, and all were homogeneous to within 15%. For the more inhomogeneous samples, several points with different water contents were tracked during an experiment.

Doubly polished glass wafers were placed in the hotspot of muffle furnaces for H_2O and OH interconversion. The wafers were taken out and quenched after a designated time, analyzed for H_2O and OH concentrations, and then placed back in the furnace to react further. Experiments were conducted in two horizontal furnaces equipped with automatic temperature controllers. Temperature fluctuations were ≤ 2 °C. Temperature gradients were <0.1 °C/mm in the vicinity of the hotspot. Glass wafers were quenched by pulling them into ice water. This procedure results in a quenching time scale on the order of 1 s, depending on the thickness of the sample.

The experiments are aimed at determining the rate of the overall reaction

$$H_2O + O \rightleftharpoons 2OH \quad (1)$$

where O is an anhydrous O atom and OH is bonded to Al, Si, or other ions (but not H). This involves monitoring the change of concentrations of H_2O and OH with time during experiments for a given sample. Whether or not equilibrium is reached in a particular experiment, we define

$$Q = \frac{[OH]^2}{[H_2O][O]} \quad (2)$$

where [OH], [H_2O], and [O] are the mole fractions of these species defined on a single O basis (Stolper, 1982b, 1989). When equilibrium is reached, the expression on the right-hand side of Equation 2 is referred to as K. Because mole fractions instead of activities are used in the expression, K is expected to depend on total water content (unless there are only these three distinguishable O species in the melt or glass and they mix ideally). The variation of Q with time characterizes how equilibrium is reached. Glass wafers for each set of experiments were usually chosen so that the initial Q differed from the value of K at the experimental temperature, as estimated from

TABLE 1. Experimental data on speciation evolution with time for natural rhyolitic glasses

Sample	T (°C)	t (min)	H_2O + OH (wt%)	H_2O (wt%)	OH (wt%)	$-\ln Q$	Comments
A-D2C,* 2.3% water, 0.83 mm thick, microphenocrysts, bubbles							
0	550**	equil	2.29 ± 0.03	1.08	1.20	2.291 ± 0.022	4, p.e.(550)
1	600	0.33	2.21 ± 0.08	0.962	1.25	2.102 ± 0.024	2, e, q
2	600	0.67	2.27 ± 0.07	0.996	1.27	2.095 ± 0.025	2, e, q
B-D6A,* 1.4% water, 1.74 mm thick, bubbles							
0	550**	equil	1.435 ± 0.009	0.546	0.891	2.228 ± 0.018	3, p.e.(550)
1	600	2	1.41 ± 0.04	0.479	0.927	2.013 ± 0.037	2, e
C-D1C, 1.0% water, 3.3 mm thick, bubbles, microphenocrysts, bands							
0	—	—	1.09	0.441	0.653	2.642	1, n
1	600	1	1.07	0.366	0.709	2.287	1
2	600	3	1.06	0.308	0.752	1.995	1
3	600	6	1.04	0.298	0.747	1.976	1, e
4	600	10	1.04	0.296	0.746	1.973	1, e
E-D2A, 0.86% water, 3.42 mm thick, bubbles, microphenocrysts, bands							
0	—	—	0.847	0.196	0.651	1.837	1, n
1	600	1	0.862	0.219	0.643	1.974	1
2	600	3	0.862	0.215	0.647	1.944	1
3	600	6	0.861	0.214	0.647	1.938	1
4	600	10	0.858	0.210	0.648	1.914	1, e
G-D4, 0.8% water, 2.43 mm thick, microphenocrysts, bands							
0	—	—	0.791	0.260	0.531	2.529	1, n
1	600	1	0.811	0.262	0.550	2.468	1
2	600	3	0.775 ± 0.005	0.199	0.576	2.098 ± 0.018	2
3	600	6	0.770	0.177	0.593	1.923	1
4	600	10	0.770 ± 0.001	0.176	0.594	1.912 ± 0.018	2, e
A-D2C, 2.3% water, 0.83 mm thick, microphenocrysts, bubbles							
0	—	—	2.36 ± 0.05	1.19	1.17	2.444 ± 0.025	2, n
1	550	0.33	2.36 ± 0.09	1.16	1.20	2.371 ± 0.001	2
2	550	0.83	2.31 ± 0.09	1.12	1.18	2.362 ± 0.027	2
3	550	1.50	2.29 ± 0.04	1.08	1.21	2.288 ± 0.023	3, e
4	550	2.50	2.28	1.08	1.20	2.299	1, e
B-D6A, 1.4% water, 1.7 mm thick, bubbles							
0	—	—	1.434	0.542	0.892	2.215	1, n
1	550	0.33	1.458	0.558	0.900	2.225	1
2	550	0.67	1.448	0.552	0.896	2.225	1
3	550	1.00	1.459	0.569	0.890	2.268	1
4	550	1.50	1.451	0.562	0.890	2.255	1
5	550	2.00	1.454	0.564	0.890	2.258	1
6	550	3.00	1.431	0.545	0.886	2.233	1
7	550	4.00	1.440	0.546	0.894	2.218	1, e
8	550	7.50	1.435	0.547	0.888	2.234	1, e
B-D1B*-1,† 1.3 mm thick, piece 1 from B-D1B. Heated at 600 °C for 30 s							
0	600**	—	1.276	0.422	0.854	2.055	1
1	550	0.67	1.292	0.456	0.836	2.173	1
2	550	2.00	1.294	0.460	0.835	2.184	1
3	550	4.00	1.292	0.460	0.832	2.192	1, e
4	550	10.00	1.283	0.454	0.829	2.188	1, e
B-D1B*-2,† 1.3 mm thick, piece 2 from B-D1B							
0	500**	equil	1.331	0.525	0.806	2.389	1, p.e.(500)
1	550	0.67	1.328	0.498	0.830	2.276	1
2	550	2.00	1.312	0.472	0.840	2.199	1
3	550	4.00	1.306 ± 0.033	0.466	0.840	2.185 ± 0.004	2, e
4	550	10.00	1.302	0.463	0.839	2.183	1, e
B-D1B*-3,† 0.97 mm thick, piece 3 from B-D1B. Both sides were polished down by ~160 μm. This piece was heated at 600 °C for 10 s							
0	600**	—	1.285	0.440	0.846	2.114	1
1	550	0.33	1.301	0.459	0.841	2.169	1
2	550	0.83	1.297	0.461	0.836	2.186	1
3	550	1.33	1.293	0.469	0.824	2.230	1
4	550	2.50	1.290	0.459	0.831	2.192	1
B-D1B*-4,† 0.975 mm, piece 4 from B-D1B. Both sides polished down by ~160 μm							
0	500**	equil	1.302	0.509	0.793	2.389	1, p.e.(500)
1	550	0.33	1.303	0.486	0.816	2.286	1
2	550	0.83	1.295	0.474	0.821	2.250	1
3	550	1.33	1.292	0.475	0.817	2.260	1
4	550	2.50	1.272	0.452	0.819	2.207	1

TABLE 1.—*Continued*

Sample	T (°C)	t (min)	H_2O + OH (wt%)	H_2O (wt%)	OH (wt%)	$-\ln Q$	Comments
			F-D4B, point 1, 0.80% water, 1.8 mm thick, microphenocrysts, bands, few bubbles				
0	—	—	0.774	0.204	0.570	2.143	1, n
1	550	0.33	0.801	0.226	0.575	2.229	1
2	550	0.67	0.805	0.228	0.577	2.234	1
3	550	1.17	0.810	0.231	0.579	2.240	1
4	550	1.67	0.813	0.235	0.578	2.257	1
5	550	2.33	0.798	0.221	0.577	2.203	1
6	550	3.33	0.802	0.220	0.582	2.178	1
7	550	4.83	0.789	0.212	0.577	2.157	1
8	550	7.08	0.806	0.219	0.587	2.155	1
9	550	12.00	0.804	0.214	0.590	2.126	1, e
10	550	22.00	0.792	0.208	0.584	2.115	1, e
			F-D4B, point 2, 0.76% water, 1.8 mm thick, microphenocrysts, bands, few bubbles				
0	—	—	0.757	0.193	0.564	2.108	1, n
1	550	0.33	0.780	0.214	0.545	2.211	1
2	550	0.67	0.778	0.212	0.565	2.203	1
3	550	1.17	0.775	0.213	0.562	2.215	1
4	550	1.67	0.773	0.210	0.563	2.197	1
5	550	2.33	0.772	0.209	0.564	2.192	1
6	550	3.33	0.770	0.204	0.566	2.161	1
7	550	4.83	0.762	0.198	0.564	2.141	1
8	550	7.08	0.768	0.202	0.566	2.152	1
9	550	12.00	0.764	0.196	0.568	2.115	1, e
10	550	22.00	0.760	0.193	0.567	2.104	1, e
			B-D1B, 1.3% water, 1.4 mm thick, bubbles				
0	—	—	1.310 ± 0.016	0.464	0.846	2.168 ± 0.030	3, n
1	500	5	1.339 ± 0.010	0.511	0.828	2.307 ± 0.014	3
2	500	10	1.323	0.512	0.810	2.354	1
3	500	20	1.335	0.523	0.812	2.371	1
4	500	50	1.322 ± 0.037	0.514	0.808	2.360 ± 0.008	3
			Both sides polished down for 50 μm				
4P	500	50	1.329 ± 0.028	0.523	0.807	2.382 ± 0.004	3, e
5	500	110	1.335	0.527	0.808	2.387	1, e
			C-D2A, 1.1% water, 2.9 mm thick, bubbles, microphenocrysts, bands				
0	—	—	1.076 ± 0.007	0.432	0.644	2.646 ± 0.019	3, n
1	500	5	1.097 ± 0.007	0.433	0.664	2.588 ± 0.013	3
2	500	10	1.079	0.414	0.665	2.541	1
3	500	20	1.069	0.399	0.670	2.491	1
4	500	50	1.057	0.376	0.681	2.395	1
5	500	110	1.056	0.372	0.684	2.378	1, e
			D-D1, point 1, 0.9% water, 2.4 mm thick, microphenocrysts, bubbles				
0	—	—	0.893	0.204	0.688	1.767	1, n
1	500	5	0.912	0.246	0.666	2.019	1
2	500	10	0.923	0.261	0.662	2.089	1
3	500	20	0.928	0.273	0.654	2.159	1
4	500	50	0.928	0.291	0.637	2.276	1
5	500	110	0.928	0.301	0.627	2.341	1, e
			D-D1, point 2, 1.0% water, 2.4 mm thick, microphenocrysts, bubbles				
0	—	—	0.952	0.232	0.720	1.803	1, n
1	500	5	0.987	0.286	0.702	2.063	1
2	500	10	0.986	0.299	0.687	2.150	1
3	500	20	0.991	0.311	0.680	2.212	1
4	500	50	1.007	0.335	0.672	2.308	1
5	500	110	1.002	0.341	0.662	2.358	1, e
			E-D1A, 0.9% water, 3.46 mm thick, bubbles, microphenocryst, bands				
0	—	—	0.867	0.205	0.663	1.845	1, n
1	500	5	0.893	0.243	0.650	2.058	1
2	500	10	0.894	0.250	0.645	2.098	1
3	500	20	0.897	0.257	0.640	2.140	1
4	500	50	0.895	0.270	0.625	2.237	1
5	500	110	0.903	0.283	0.620	2.302	1, e
			F-D3B, 0.8% water, 3.9 mm thick, microphenocryst, bands, few bubbles				
0	—	—	0.7958 ± 0.0007	0.209	0.587	2.110 ± 0.010	2, n
1	500	5	0.816 ± 0.002	0.230	0.586	2.208 ± 0.003	2
2	500	10	0.817	0.229	0.588	2.197	1
3	500	20	0.811	0.226	0.584	2.198	1
4	500	50	0.809	0.230	0.579	2.235	1
5	500	110	0.821	0.244	0.577	2.302	1, e

TABLE 1.—*Continued*

Sample	T (°C)	t (min)	H_2O + OH (wt%)	H_2O (wt%)	OH (wt%)	$-\ln Q$	Comments
			G-D1A, 0.77% water, 1.3 mm thick, microphenocryst, bands few bubbles				
0	—	—	0.766	0.238	0.528	2.456	1, n
1	500	5	0.783	0.255	0.528	2.525	1
2	500	10	0.778	0.251	0.527	2.511	1
3	500	20	0.781	0.250	0.531	2.494	1
4	500	50	0.770	0.236	0.533	2.426	1
5	500	110	0.761	0.231	0.530	2.418	1
			H-D1B, point 1, 0.78% water, 2.31 mm thick, bands, few microphenocrysts, few bubbles				
0	—	—	0.773	0.273	0.500	2.702	1, n
1	500	5	0.790	0.291	0.500	2.764	1
2	500	10	0.793	0.291	0.502	2.753	1
3	500	20	0.789	0.285	0.504	2.730	1
4	500	50	0.786	0.275	0.510	2.667	1
5	500	110	0.778	0.266	0.512	2.628	1
			H-D1B, point 2, 0.72% water, 2.31 mm thick, bands, few microphenocrysts, few bubbles				
0	—	—	0.696	0.230	0.466	2.674	1, n
1	500	5	0.739	0.257	0.482	2.712	1
2	500	10	0.740	0.257	0.482	2.714	1
3	500	20	0.757	0.265	0.492	2.703	1
4	500	50	0.714	0.236	0.478	2.646	1
5	500	110	0.712	0.231	0.481	2.613	1
			B-D5A, 0.5% water, 1.1 mm thick				
0	—	—	0.523 ± 0.026	0.072	0.453	1.565 ± 0.082	2, n
1	500	2	0.532 ± 0.004	0.078	0.454	1.648 ± 0.007	2
2	500	5	0.532 ± 0.009	0.079	0.452	1.668 ± 0.044	2
3	500	10.2	0.528 ± 0.011	0.081	0.448	1.705 ± 0.014	2
4	500	20.2	0.527 ± 0.011	0.081	0.446	1.717 ± 0.052	3
5	500	50.2	0.525 ± 0.018	0.086	0.439	1.813 ± 0.020	3
			Both sides polished down by 50 μm				
5P	500	50.2	0.526 ± 0.025	0.085	0.441	1.794 ± 0.061	3
6	500	110.2	0.533 ± 0.017	0.091	0.442	1.857 ± 0.023	2
			E-D3, 0.8% water, 2.30 mm thick, bubbles, microphenocryst, bands				
0	—	—	0.848 ± 0.008	0.197	0.651	1.843 ± 0.028	5, n
1	482	5	0.874 ± 0.018	0.232	0.642	2.037 ± 0.021	3
2	482	11	0.872 ± 0.025	0.234	0.638	2.056 ± 0.026	3
3	482	34	0.875 ± 0.021	0.247	0.628	2.143 ± 0.003	3
4	482	94	0.883 ± 0.022	0.267	0.616	2.255 ± 0.018	3
5	482	254	0.882 ± 0.025	0.279	0.603	2.342 ± 0.024	3
6	482	674	0.870 ± 0.020	0.284	0.586	2.417 ± 0.016	3
			H-D2A, point 1, 0.80% water, 3.25 mm thick, bands, few microphenocrysts, few bubbles				
0	—	—	0.796	0.290	0.506	2.734	1, n
1	482	5	0.806	0.298	0.508	2.759	1
2	482	11	0.802	0.294	0.508	2.744	1
3	482	34	0.812	0.300	0.513	2.741	1
4	482	94	0.816	0.297	0.519	2.710	1
5	482	254	0.804	0.284	0.521	2.656	1
6	482	674	0.796	0.269	0.528	2.578	1
			H-D2A, point 5, 0.88% water, 3.24 mm thick bands, few microphenocrysts, few bubbles				
0	—	—	0.868	0.332	0.536	2.756	1, n
1	482	5	0.891	0.352	0.538	2.807	1
2	482	11	0.867	0.336	0.532	2.783	1
3	482	34	0.888	0.346	0.541	2.777	1
4	482	94	0.888	0.338	0.551	2.717	1
5	482	254	0.881	0.325	0.557	2.656	1
6	482	674	0.849	0.289	0.560	2.529	1
			H-D2A, point 7, 0.77% water, 3.25 mm thick, bands, few microphenocrysts, few bubbles				
0	—	—	0.733	0.250	0.484	2.678	1, n
1	482	5	0.813	0.303	0.510	2.767	1
2	482	11	0.797	0.288	0.509	2.718	1
3	482	34	0.781	0.278	0.503	2.708	1
4	482	94	0.798	0.286	0.513	2.695	1
5	482	254	0.772	0.266	0.506	2.654	1
6	482	674	0.768	0.257	0.511	2.595	1
			A-D2C, 0.850 mm thick, microphenocrysts, bubbles, equilibrated at 600 °C				
0	—	—	2.217	0.964	1.253	2.095	1
1	400	2.5	2.316	1.168	1.148	2.463	1
2	400	5	2.338	1.208	1.130	2.529	1

TABLE 1.—*Continued*

Sample	T (°C)	t (min)	H_2O + OH (wt%)	H_2O (wt%)	OH (wt%)	$-\ln Q$	Comments
3	400	10	2.346	1.245	1.101	2.612	1
4	400	20	2.366	1.297	1.069	2.711	1
			A-D2D, 0.875 mm thick, microphenocrysts, bubbles, heated at 500 °C for 10 min				
0	—	—	2.545 ± 0.027	1.320	1.225	2.453 ± 0.024	2
1	400	1	2.572	1.388	1.184	2.571	1
2	400	2	2.587	1.419	1.169	2.619	1
3	400	5	2.603 ± 0.046	1.453	1.149	2.677 ± 0.004	2
4	400	10	2.611	1.483	1.129	2.733	1
5	400	20	2.626	1.520	1.106	2.799	1
6	400	40	2.622	1.540	1.082	2.855	1
				Variable T, D-D1			
0	500	110	0.946	0.305	0.641	2.311	1, e
1	450	115	0.950	0.311	0.639	2.337	1
2	400	120	0.946	0.311	0.635	2.349	1
3	350	125	0.943	0.308	0.635	2.339	1
4	300	130	0.945	0.310	0.635	2.345	1
5	250	135	0.943	0.309	0.634	2.345	1
6	200	145	0.936	0.305	0.631	2.341	1
7	in liquid N_2		0.941	0.307	0.634	2.340	1

Note: sample numbers are simplified for clarity. The following key can be used to compare samples used in this study and those in Newman et al. (1986, 1988) and Zhang et al. (1991): A = MC84-bb-3a; B = MC84-bb-3b; C = POB82-10; D = MC84-bb-6b1; E = POB82-1; F = KS; G = MN85-jh; and H = MC85-Ka. The numbers that follow are used to identify the different pieces in this study. Some of these pieces are cut from the same chunk of glass, others are from different chunks but the same bed of flow. H_2O + OH wt% and $-\ln Q$: If there were two or more analyses, 2σ errors are also given. Comments: The first number indicates the number of analyses; n = natural, untreated obsidian glass as starting material; e = equilibrium believed to be reached; p.e.(550) = preequilibrated at 550 °C; q = there may be a quench effect.

* The starting glass wafer has been heated before.

** Note temperature change.

† Pieces are cut from B-D1B, which has been equilibrated at 500 °C. Two of them (pieces 2 and 4) are directly used in the 550 °C experiments, and two others were first heated at 600 °C (but did not reach equilibrium) and then heated at 550 °C.

previous experimental studies (Zhang et al., 1991). However, in some cases, glass wafers with Q similar to the expected K were used to examine how Q approached K under these circumstances. Although the glasses are metastable, there was no appreciable crystallization on the time scale of the experiments. Furthermore, the equilibrium condition is robust and reversible. We therefore conclude that the kinetic data are robust and not affected by the metastability of the glass.

Since dehydration occurs during heating, surficial layers of the wafers were ground off and repolished whenever estimates of dehydration (based on Zhang et al., 1991) predicted a $\geq 0.5\%$ relative change in concentration measurements. The measured points were always far enough from edges of polished faces so that analyses were unaffected by loss of water from these edges.

ANALYTICAL METHODS

Before the experiment and after each heating-quenching cycle, one or more spots in the polished wafer were analyzed by infrared spectroscopy with a Nicolet 60SX FTIR, in general following the procedures of Newman et al. (1986). Round apertures (100–600 μm in diameter, depending on the size of the wafer) were used to delimit the infrared beam. The H_2O and OH concentrations were determined from the peak heights of the absorption bands at 5230 and 4520 cm^{-1} using the molar absorptivities of Newman et al. (1986) for rhyolitic glasses and calculated glass density (Silver et al., 1990). The OH concentrations are reported as the weight percent of water present as OH. Total water contents were obtained by summation of the concentrations of these two species. For the albitic glass, H_2O and OH concentrations were determined using the molar absorptivities and glass densities of Silver and Stolper (1989).

The relative precision of measured H_2O and OH concentrations is estimated in two ways: one is based on an internal standard and the other on repeated analyses of relatively homogeneous samples. An internal standard (E-D2; 0.86% water with a thickness of 3.45 mm) was analyzed 13 times along with the samples of this study. In addition to these multiple analyses of the internal standard, many samples were analyzed on several nearby points (Tables 1 and 2). Based on these analyses, 2σ relative errors of ~1% have been assigned for H_2O and OH, except when the absorbance is <0.1, in which case the 2σ relative error is $>1\%$ and is estimated on the basis of the quality of each spectrum (often the 2σ absolute error is ~0.001 in absorbance for the 5230 and 4520 cm^{-1} bands). (All errors below are given at the 2σ level.) Errors on Q are based on statistical propagation of the uncertainties on OH and H_2O (a typical error for $\ln Q$ is 0.022). For inhomogeneous samples, the observed variation in Q is similar to that of more homogeneous samples even though water (and H_2O and OH) content varies.

Accuracy of the measurements depends on the accuracy of the molar absorptivities (ϵ_{5230} and ϵ_{4520}) calibrated by Newman et al. (1986). Table 1 shows that for many

TABLE 2. Experimental data of speciation evolution with time for a synthetic albitic glass

Sample	T (°C)	t (min)	H_2O + OH (wt%)	H_2O (wt%)	OH (wt%)	$-\ln Q$	Comments*
			500 °C, 0.77 mm thick				
0	—	—	1.008	0.150	0.858	1.005	1
1	500	3	1.012	0.118	0.895	0.676	1
2	500	6	1.016	0.130	0.886	0.792	1
3	500	10	1.022	0.140	0.882	0.879	1
4	500	15	1.031	0.151	0.880	0.956	1
5	500	20	1.025 ± 0.001	0.157	0.868	1.030 ± 0.004	2
6	500	30	1.027	0.165	0.862	1.088	1
7	500	40	1.020	0.169	0.851	1.140	1
8	500	62	1.029	0.181	0.848	1.217	1
9	500	92	1.020	0.187	0.832	1.286	1
10	500	127	1.020	0.196	0.824	1.349	1
11	500	180	1.019	0.201	0.818	1.391	1
11P	500	180	1.020	0.202	0.818	1.394	1
			600 °C, 0.65 mm thick**				
0	—	—	1.017 ± 0.004	0.199	0.817	1.384 ± 0.014	3
1	600	0.5	1.008	0.188	0.820	1.321	1
2	600	1.5	1.004	0.176	0.828	1.236	1
3	600	3	0.998	0.172	0.826	1.218	1
4	600	8	0.980 ± 0.016	0.163	0.817	1.188 ± 0.028	5, e?
			550 °C, 0.65 mm thick**				
0	—	—	0.980 ± 0.016	0.163	0.817	1.188 ± 0.028	5
1	550	1	0.986 ± 0.001	0.174	0.812	1.265 ± 0.006	2
2	550	3	0.984 ± 0.003	0.179	0.805	1.307 ± 0.006	2
3	550	6	0.980 ± 0.010	0.182	0.798	1.341 ± 0.034	2
4	550	12	0.986 ± 0.005	0.187	0.799	1.369 ± 0.006	2
5	550	20	0.980 ± 0.000	0.188	0.791	1.394 ± 0.021	2, e?

Note: the starting albitic glass (ABC-26) was quenched from 1400 °C and 20 kbar in a piston-cylinder apparatus. It was held at 500 °C, then at 400, 450, 600, and 550 °C. This table follows the sequence of the experiments, not descending or ascending order of temperature.

* Comments are the same as in Table 1.

** Heated at 400 °C for 61 min and 450 °C for 169 min, but changes in Q were insignificant.

of the samples the total water concentration calculated using the calibration of Newman et al. (1986) appears to vary up to 5% (relative) with progressive heat treatment. The apparent variation in total water content correlates with the variation in the ratio of the peak heights of the 5230 and 4520 cm^{-1} bands. Such variations have been observed before and attributed either to errors in the molar absorptivities of the two bands or to their dependence on thermal history of the glasses (Skirius et al., 1990; Zhang et al., 1991). Assuming (1) total water content is constant during heat treatment (since diffusive loss is negligible; Zhang et al., 1991) and (2) ϵ_{5230} and ϵ_{4520} are independent of thermal history, the $\epsilon_{5230}/\epsilon_{4520}$ ratio can be obtained from our data by recasting

$$c = \frac{18.015}{\rho d}\left(\frac{A_{5230}}{\epsilon_{5230}} + \frac{A_{4520}}{\epsilon_{4520}}\right) \quad (3)$$

(Newman et al., 1986) into

$$A_{5230} = \frac{\rho d c}{18.015}\epsilon_{5230} - \frac{\epsilon_{5230}}{\epsilon_{4520}}A_{4520} \quad (4)$$

where A stands for absorbance, ϵ for molar absorptivity, ρ for density, d for the thickness, and c for the total water content. From linear regressions of A_{5230} vs. A_{4520} for each sample heated at different temperatures, an $\epsilon_{5230}/\epsilon_{4520}$ ratio of 1.6 ± 0.3 is obtained from all the samples studied, whereas Newman et al. (1986) obtained $\epsilon_{5230}/\epsilon_{4520}$ = 1.61/1.73 = 0.93 for similar rhyolitic glasses. The results suggest that either the molar absorptivities of Newman et al. (1986) have relatively large errors or the molar absorptivities depend on the thermal history. Without a complete understanding of the causes of these variations, caution must be exercised in the interpretation of small change in speciation. In this report, we still use the molar absorptivities of Newman et al. (1986) for consistency with previous reports and because we do not have a complete and reliable redetermination of the molar absorptivities. If the change in apparent total water content with heat treatment is due to errors in the molar absorptivities of Newman et al. (1986), but the molar absorptivities are independent of the thermal history of the glass, then reported values of Q are affected by a roughly constant factor, and the relative variations in Q are unaffected. In contrast, if molar absorptivities also depend on the thermal history, then small variations in Q could be artifacts of our assumption of constant molar absorptivities. However, the factor of two variations in Q observed in this study are unlikely a result of uncertainties in the molar absorptivities. Because of the robustness of the parameter Q (i.e., its insensitivity to small variations in water content, whether due to sample heterogeneity or to uncertainty in molar absorptivities) as a monitor of interconversion of OH and H_2O by Reaction 1, results and interpretations throughout this paper focus on the evolution of this parameter during heat treatment.

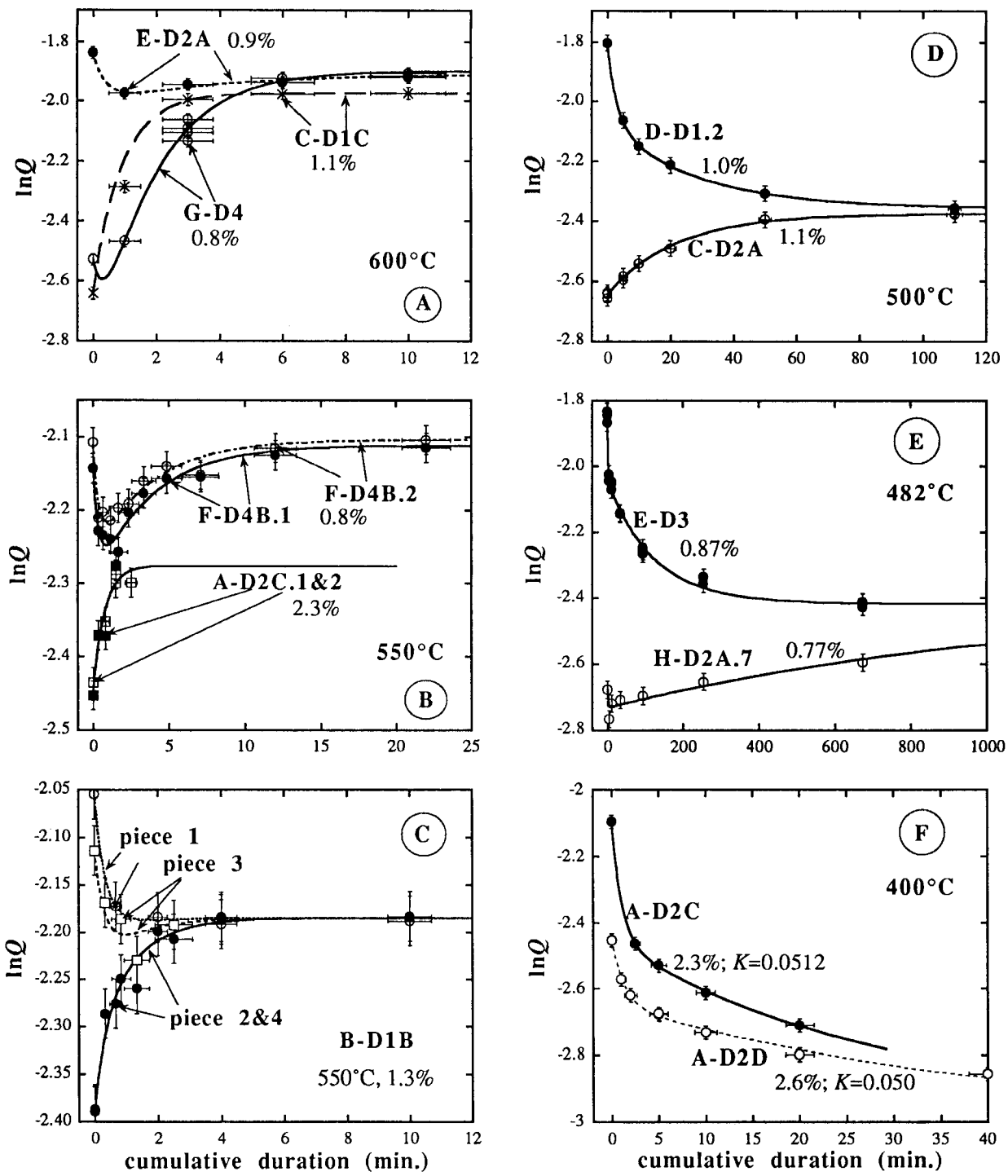

Fig. 1. Experimental data (with 2σ error bars) showing how Q approaches K as a function of time for rhyolitic glasses and fitting results. Q vs. t data are fit because Q is a robust parameter. The fit minimizes $\Sigma\, d_i^2$. Uncertainties on experimental duration are estimated from heating-up time (which contributes most of the uncertainty) and quench time, both depending on the thickness of the sample. Note that equilibrium was not reached for the samples at 400 °C or for H-D2A at 482 °C. A–F are for different samples and different temperatures.

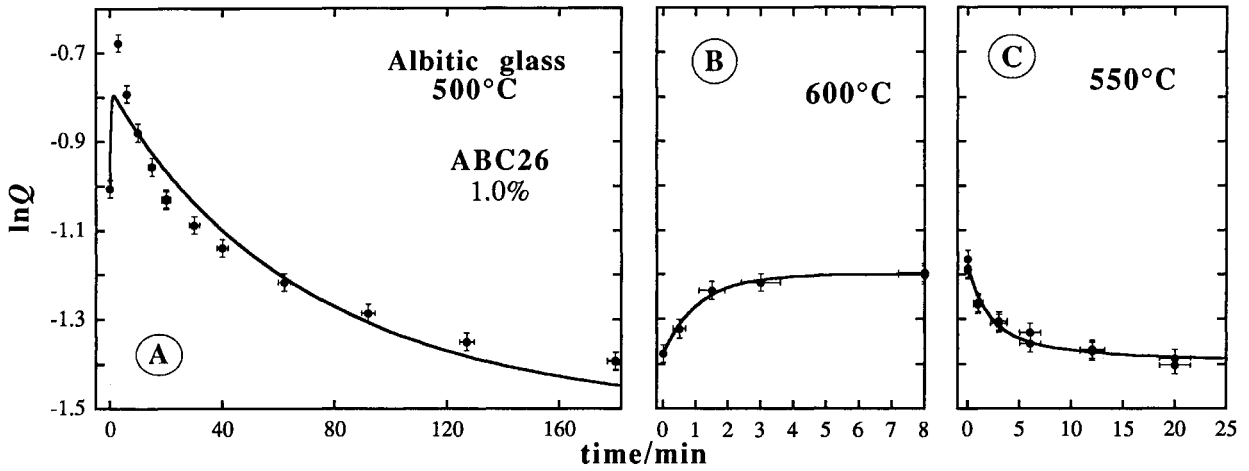

Fig. 2. Experimental data (with 2σ error bars) and fitting results for a synthetic albitic glass. Equilibrium was not reached at 500 °C. (**A**) Heating experiments at 500 °C for a glass quenched from 20 kbar and 1400 °C; (**B**) heating experiments at 600 °C for the same wafer after the 500 °C experiments; (**C**) heating experiments at 550 °C for the same wafer after equilibration at 600 °C.

Experimental results

All experimental data are reported in Tables 1 and 2. Several representative sets of experiments showing the time dependence of Q and the reversed approach to its equilibrium value, K, are shown in Figure 1 for rhyolitic glasses and Figure 2 for albitic glass. Many samples approach equilibrium monotonically and smoothly on a ln Q vs. t plot (for example, D-D1.2 and C-D2A at 500 °C, Fig. 1D). All samples that were first equilibrated at one temperature and then were held at a second temperature show such a monotonic approach to the new K (such as B-D1B, pieces 2 and 4 in Fig. 1C; albitic glass at 550 °C in Fig. 2). For a given T and total water content, the same value of K is reached for samples approaching equilibrium from both sides (i.e., from inital values of Q higher or lower than K; see Fig. 1A, 1C, and 1D). However, for samples with different water content, different K values are reached at the same T (compare F-D4B in Fig. 1B, A-D2C in Fig. 1B, and B-D1B in Fig. 1C), reflecting the dependence of K on water content.

An interesting and important feature of the data is that the approach of Q to K is not always monotonic. For example, for sample F-D4B at 550 °C, Q first decreased and then increased toward the equilibrium K (Fig. 1B). For the synthetic albitic glass at 500 °C, Q first increased and then decreased to the equilibrium K (Fig. 2A). Several observations offer strong evidence that the nonmonotonic behavior is real and not a mere artifact of our imperfect knowledge of molar absorptivities and their possible dependence on thermal history: (1) the magnitudes of these seemingly anomalous phenomena, (2) their occurrence in experiments approaching K from both above and below, and (3) their occurrence in both synthetic albitic and natural rhyolitic glasses. This complexity of nonmonotonic behavior suggests that the approach to equilibrium involves more than the simple forward and backward processes of Reaction 1.

Discussion

Relaxation time scale

The time to reach equilibrium decreases with increasing temperature and increasing water content. For example, sample C-D1C (1.1% total water) reached equilibrium speciation in ~3 min at 600 °C (Fig. 1A), but C-D2A (another piece of the same chunk of glass) of similar water content reached equilibrium in ~100 min at 500 °C (Fig. 1D). At 600 °C, sample A-D2C (2.3% total water) reached equilibrium speciation in ~0.4 min, but C-D1C (1.1% total water) required 3 min, and G-D4 (0.8% total water) required ~6 min. In general, the time for Reaction 1 to reach equilibrium in albitic glass is comparable to that in rhyolitic glass, except at 500 °C where equilibrium was not reached.

The relaxation time scale, τ_r, defined as the time required for $[H_2O] - [H_2O]_e$ (i.e., the difference between the measured and the equilibrium concentration of H_2O) to decrease to 1/e of its original value, is used to quantify the time scale to reach equilibrium. For sequences of experiments in which Q approaches K monotonically, the $[H_2O]$ vs. t data have been fitted by

$$[H_2O] = A + Be^{-t/\tau_r} \quad (5)$$

(or Q vs. t using $Q = A + Be^{-t/\tau_r}$). The τ_r value from the fit is the relaxation time scale. The τ_r obtained from fitting $[H_2O]$ vs. t is slightly different from that obtained by fitting Q vs. t, but the difference is small in comparison with uncertainties in the best-fit τ_r. Although many fits to monotonic profiles are good, the existence of nonmonotonic profiles and the poor fits to some monotonic profiles demonstrate that Equation 5 does not adequately describe our data. These details will be discussed in more detail later in this paper. Nevertheless, we choose to use the τ_r obtained by the fits as a rough model-independent estimate of the relaxation time scale for the monotonic

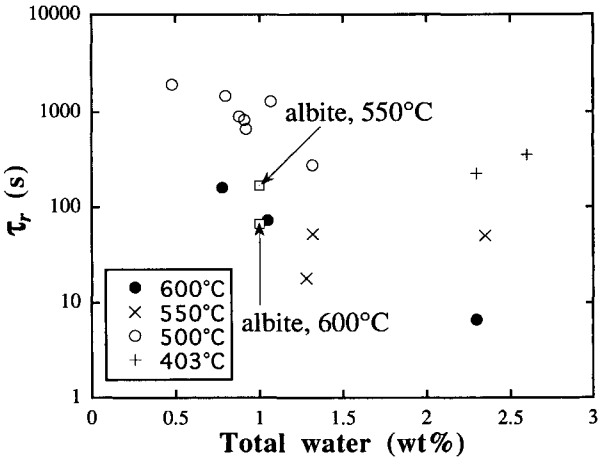

Fig. 3. Relaxation time scale of Reaction 1 (based on isothermal experiments that approach equilibrium monotonically) as a function of temperature and total water content. The relaxation time scale is obtained by fitting a simple exponential function through the Q vs. t data. Solid circles are for 600 °C data, Xs for 550 °C, open circles for 500 °C, and plus signs for 403 °C. Two points for an albitic glass (ABC-26) with ~1.0% water are marked.

trends. Best-fit values of τ_r are plotted in Figure 3 as a function of temperature and water content. Although there is much scatter, probably reflecting the simplistic approach to determining the relaxation time scale, the trends in Figure 3 illustrate that τ_r decreases with both increasing total water content and temperature. Relaxation time scales of the albitic glasses are comparable with those of rhyolitic glasses at similar temperatures and water content (Fig. 3). The relaxation time scales for reaction in rhyolitic glasses demonstrate that 1-atm speciation data reported in Stolper (1989) and Zhang et al. (1991) were not affected by quenching that had a time scale of ~1 s.

Since the relaxation time scales deduced above show considerable scatter, it is difficult to extrapolate from such data to infer the effect of quenching on other experiments. We therefore examined speciation data on rhyolitic glasses quenched from 850 °C reported by Silver et al. (1990) and Ihinger (1991). Two different quench methods were used and resulted in slow quench (~3 °C/s) and rapid quench (~200 °C/s) rates. Recorded Q values are different for samples of the same water content that were quenched at different rates and for samples with different water contents that were quenched at the same rate. Each recorded Q value would be the equilibrium K at some temperature (which can be calculated from Fig. 6 of Zhang et al., 1991) that is referred to as the "apparent equilibrium temperature" (T_{ae}) of the reaction. To avoid confusion, we use T_{ae} to refer to the apparent equilibrium temperature recorded by speciation based on Reaction 1 after quench, and use the fictive temperature, T_f, to refer to the glass transition temperature (Dingwell and Webb, 1990). The 2σ uncertainty on T_{ae} based on Zhang et al. (1991) is ~16 °C and is independent of the accuracy of the molar absorptivities (as long as the same molar absorptivities are used). Calculated T_{ae} values are less than the experimental temperature, 850 °C, for water contents ≥0.8% (Fig. 4), indicating that speciation is altered even during rapid quench (Dingwell and Webb, 1990). Water content, T_{ae}, and quench rate for the data in Silver et al. (1990) and Ihinger (1991) can be related by

$$T_{ae}\,(\mathrm{K}) = \frac{26200}{40.3 - \ln q - \dfrac{0.324}{0.0167 + [\mathrm{water}]}} \quad (6)$$

where q is the quench rate (in degrees Celsius per second) at $T = T_{ae}$ (q at $T = T_{ae}$ is calculated from the initial q reported in Silver et al., 1990; see caption in Fig. 4) and [water] is the molar fraction of total water on a single O basis. Equation 6 reproduces T_{ae} from the Silver et al. (1990) and Ihinger (1991) data set with a 2σ error of 34 °C. Alternatively, Equation 6 can be used to calculate quench rate from T_{ae} and water content for each sample. Calculated quench rates reproduce the experimental quench rates for this data set to within a factor of 3 [i.e., $\ln(q_{calc}/q_{obs})$ is -0.1 with 2σ error of 1.2].

From this quench rate, the relaxation time scale at $T = T_{ae}$ can be estimated. Zhang (1994) found that for five types of reactions the relaxation time scale and quench rate are related by

$$\tau_r \approx \frac{2RT_{ae}^2}{q\ \max(E_f, E_b)} \quad (7)$$

where R is the gas constant and $\max(E_f, E_b)$ is the greater of E_f (activation energy for the forward reaction) and E_b (activation energy for the backward reaction). Assuming this relation also applies to Reaction 1, relaxation time scales can be calculated from the quench rate and from the apparent equilibrium temperature recorded by the quenched speciation. Assuming $\max(E_f, E_b)/(2R) \approx 12000$ K, the calculated relaxation time scale is 0.46 ± 0.04 s for all the rapid-quench samples and 26.1 ± 1.0 s for all the slow-quench samples.

By combining Equations 6 and 7 to eliminate q, the relaxation time scale implied by a particular T_{ae} can be related to water content. Values of τ_r calculated in this way ($\tau_{r,calc}$) for the isothermal time-series experiments reported here can be compared with values obtained by fitting the time-series data to Equation 5 ($\tau_{r,fit}$) (Fig. 3). Values of τ_r calculated in these two ways are similar to $\ln(\tau_{r,calc}/\tau_{r,fit}) = 0.0$ with 2σ error of 2.6. We consider these independent approaches to estimating the relaxation time scale to be in reasonable agreement; the large uncertainty probably reflects the complexity of the reaction as evidenced from the poor fit of some of the isothermal experiments to a simple exponential approach to equilibrium.

The isothermal time-series experiments reported here provide relaxation time scales and a direct estimate of quench effects for the low-temperature experiments. They also constrain the reaction mechanism, which is necessary before speciation data can be used to infer complex thermal histories. However, owing to our imperfect understanding of the reaction mechanism at present, these experimental data show large scatter in τ_r. The quench

rate experiments of Silver et al. (1990) and Ihinger (1991), on the other hand, show less scatter and are more reliable as the basis of interpolation and extrapolation for estimating relaxation time scales as functions of quench rate and water content. Therefore, the two approaches complement each other.

The effect of quenching in reported experimental data

Knowledge of the relaxation time scale is necessary for evaluating the time scale required to reach the equilibrium speciation in an experiment, as well as for determining the conditions under which species concentrations can be preserved upon quenching from high temperature. If Equation 6 is used as the basis for extrapolation, then for quenched samples to achieve a T_{ae} of 850 °C requires quench rates of 200 °C/s for 0.61% water, 2000 °C/s for 1% water, 5×10^4 °C/s for 2%, and even higher quench rates for greater water content. Under typical rapid-quench conditions with a quench rate of the order 200 °C/s, it will not be possible to preserve species concentrations from 850 °C for samples with ≥0.8% water. We conclude that speciation is altered in rhyolitic glasses quenched from 850 °C or higher temperature (Silver et al., 1990) even for the most rapid quenches yet achieved. Furthermore, we conclude that natural rhyolitic glasses and glass inclusions do not record water speciation of the preeruptive melt. These conclusions have also been demonstrated by Ihinger (1991) and were anticipated by the modeling of Dingwell and Webb (1990), who estimated time scales for Reaction 1 from glass relaxation theory. As for the role of the kinetics of Reaction 1 in converting OH groups to H_2O molecules and thus providing ingredients for bubble growth and degassing, the relaxation time scale at 850 °C is ≤2 ms for water contents ≥2%; therefore, conversion of OH into H_2O may be regarded as instantaneous as long as water content is high, and it does not limit bubble growth and degassing.

Figure 4 may be used to evaluate quench effects of lower-temperature and 1-atm experiments, but one may also use Equation 6 or our isothermal data. For experiments quenched at the same rate as the rapid-quench experiments in Figure 4, the quench effect is equivalent to a temperature effect of ≤6 °C as long as experimental T is lower than T_{ae} in Figure 4 by ≥20 °C (calculation based on Zhang, 1994, ignoring the complexity of the reaction mechanism). Therefore, for an experimental temperature of 600 °C, the quench effect is negligible for a total water content ≤2.0%; for an experimental temperature of 550 °C, the quench effect is negligible for a total water content ≤3.2%. By extrapolation, for an experimental temperature of 500 °C, the quench effect is negligible for total water content ≤5.5%. Quench rates of 1-atm experiments are slightly greater than the rapid quench in cold-seal vessels because during quenching in 1-atm experiments, the sample is in direct contact with water and the water to sample ratio is large. Therefore, we conclude that the experimental data of Stolper (1989; except for a few 5 kbar experiments) and Zhang et al. (1991) are not significantly influenced by quenching, and

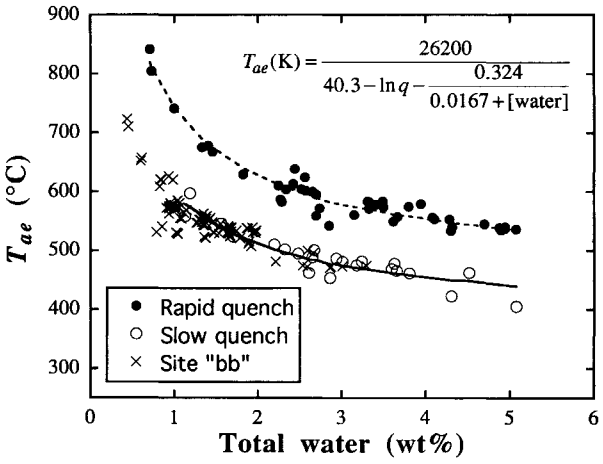

Fig. 4. Apparent equilibrium temperature vs. total water content for natural rhyolitic glasses and rhyolitic glasses quenched from 850 °C. Solid circles are for glasses after rapid quench (initial quench rate is 200 °C/s), open circles are for glasses after slow quench (initial quench rate is 3.3 °C/s), and Xs are for natural pyroclastic glasses from conformable tephras in a pit dug at site "bb" of the Mono Craters (including high precision data of Newman et al., 1988; and data from this work). These natural glasses follow the same trend as experimental glasses quenched by compressed air flow (slow quench). The apparent equilibrium temperature of experimental charges can be related to the total water content and the quench rate using an empirical equation shown in the figure. The fit of the equation to the data is shown as dashed line for rapid quench and solid line for slow quench samples. The quench rate for each sample in the equation is that at $T = T_{ae}$ of the sample and is calculated from the initial quench rate (at T_0 = 850 °C), assuming that the temperature approached room temperature exponentially; i.e., $q = q_{850}(T - T_\infty)/(T_0 - T_\infty)$, where T_0 = 1123 K and T_∞ = 298 K.

that parameterizations of the equilibrium speciation of water in rhyolitic melts and glasses, as a function of water content and temperature based solely on these data (Zhang et al., 1991), are reliable. Although the 1-atm speciation data presented in Stolper (1989) were free from quenching effects, his parameterization of the temperature dependence of speciation is inaccurate because it incorporated data from glasses quenched from 850 °C. Appendix 1 discusses a special type of quench effect. Again, the conclusion is that the effect is unimportant.

Applicability of structural relaxation theory to Reaction 1

Dingwell and Webb (1990) presented a simple method of inferring the temperature dependence of the K of Reaction 1 using speciation data of rhyolitic glasses quenched from 850 °C (Silver et al., 1990). They correctly concluded that the quenched speciation does not reflect the speciation at 850 °C but instead reflects the speciation at T_{ae}. From the quenched speciation, they estimated the T_{ae} for each sample and obtained a relation between speciation and temperature as follows. First, they assumed that T_{ae} for Reaction 1 is the same as the fictive temperature (T_f) of the overall structural relaxation (glass transition), and

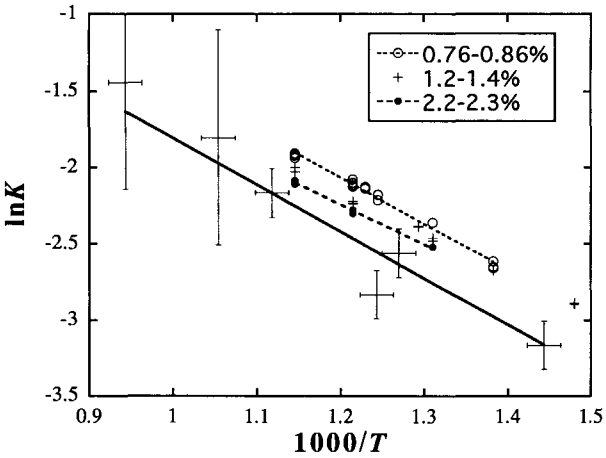

Fig. 5. Comparison of the model of Dingwell and Webb (1990) and our experimental data in terms of ln K vs. $1/T$ diagram. The heavy solid line and the points with error bars are model speciation data from Fig. 13 of Dingwell and Webb (1990). Open circles, plus signs, and solid circles are experimental data (Zhang et al., 1991; this study) for three different ranges of total water contents. The dashed lines are best-fit straight lines for the 0.76–0.86% and 2.2–2.3% total water. Errors on our experimental data are about the size of the symbols.

that the relaxation time scale (τ_r) for the reaction is the same as that for viscous flow (τ). Second, they assumed that during quench at T_f the relaxation time scale of viscous flow is $\tau = \eta/G_\infty = 8/q$ where η is the relaxed shear viscosity, G_∞ is the infinite-frequency shear modulus, and q is the quench rate in K/s. The viscosity is a function of temperature and water content and was calculated using the method of Shaw (1972). Therefore, given q and the water content for each sample, a temperature can be determined from $\eta(T, [\text{water}])/G_\infty = 8/q$, and this was the temperature they assumed to be T_{ae}. Using this T_{ae}, the speciation data, and their third assumption that K is independent of water content, Dingwell and Webb (1990) reconstructed the temperature dependence of K (shown in Fig. 5). (Dingwell and Webb have recently concluded that their third assumption is not necessary and that their calculated results actually indicate a weak dependence of K on water content; D. B. Dingwell, personal communication.)

Zhang (1994) discussed caveats in the application of structural relaxation theory to the kinetics of a specific chemical reaction from a theoretical point of view. The calculations of Dingwell and Webb (1990) can also be compared with our experimental data in two ways. One is to compare τ_r values. However, our experimental τ_r values have large uncertainties. Therefore, we choose to compare their calculated speciation with experimental results from this lab in a ln K vs. $1/T$ diagram (Fig. 5). The slope based on their calculation is similar to that from our experimental data for a given water content, and their line roughly corresponds to our extrapolated ln K vs. $1/T$ line for samples with 5% total water. However, Figure 5 shows that our ln K vs. $1/T$ data for 0.7–2.3% total water plot off their line. The offset in terms of temperature is 70–100 °C at ~0.8% total water (e.g., they would predict 696 °C for a sample equilibrated at 600 °C, and 574 °C for a sample equilibrated at 500 °C). Figure 5 also clearly demonstrates the dependence of K on total water content and the high quality of the experimental data compared with the model results of Dingwell and Webb. Therefore, the approach of Dingwell and Webb (1990) is conceptually useful and yields predicted speciation behavior that is not too far off, considering the many assumptions and the uncertainties in viscosity. However, in our view, the best way to characterize the dependence of the equilibrium of a chemical reaction on temperature, pressure, and composition, and to characterize the details of the reaction mechanisms is directly through careful experimental investigation.

Modeling experimental data

Several models of the kinetics of the reaction were considered. Because of the compositional and structural complexity of aluminosilicate melts and glasses, and given the sometimes nonmonotonic approach of Q to K, it is unlikely that any simple model will be entirely successful or that our data are sufficient to provide a complete description of this process. For example, charge-balancing cations such as Na^+ and K^+ may play roles in the reaction of H_2O molecules with anhydrous O atoms to generate OH groups (Burnham, 1975; Mysen and Virgo, 1986a, 1986b; Kohn et al., 1989a; Silver and Stolper, 1989; Mysen, 1992). Likewise, the kinetics and equilibria of reactions between bridging O atoms and H_2O molecules likely depend on the nature of the bridging O (e.g., Si-O-Si vs. Si-O-Al) and of the OH group (e.g., SiOH and AlOH) (Mysen and Virgo, 1986a, 1986b; Kohn et al., 1989a; Silver and Stolper, 1989; Zhang et al., 1990; Mysen, 1992; Sykes and Kubicki, 1993). Nonetheless it is valuable to attempt a parameterization of the data both as a guide to interpolation and extrapolation and to identify and examine some of the important parameters that will have to be incorporated into successful models.

The simplest model. The simplest model for the reaction kinetics is not successful, but it is described first to introduce the concepts on which the more complex model depends. This zero-order approximation for the reaction kinetics is based on the following two assumptions. The first is that both the forward and backward reactions are elementary ones (Lasaga, 1981). The second is that diffusion of OH is fast enough in comparison with the reaction rate, to allow for random distribution of OH groups. The reaction rate is then taken to be proportional to the number of clusters that are ready for reaction. The forward reaction rate is proportional to $[H_2O][O]$ since the number of clusters of $O\cdots H_2O$ is proportional to $[H_2O][O]$. The backward reaction rate is proportional to the number of $OH\cdots OH$ pairs. Assuming that a random distribution is always maintained during the reaction,

the number of OH pairs is approximately proportional to $[OH]^2$ (Denbigh, 1981; Eq. 16 below). The rate equation is

$$\frac{d[H_2O]}{dt} = -k_f[H_2O][O] + \frac{k_f}{K}[OH]^2 \quad (8)$$

where k_f is the rate constant for the forward reaction of Reaction 1, and the backward reaction rate constant is k_f/K because $d[H_2O]/dt = 0$ at equilibrium. This simple model fails in at least two respects to decribe the experimental data. First, it cannot account for the nonmonotonic Q vs. t curves observed under some circumstances (e.g., F samples in Fig. 1B and albite glass in Fig. 2A). Second, even in cases where Q approaches K monotonically, Equation 8 often does not fit the data well. In particular, the reaction in the first few time steps is often too rapid, compared with that in the final time steps, to be described by this simple model. Although this simple model fails, it is used as a basis for a better model that describes the experimental data well and yet is physically plausible, mathematically manageable, and sufficiently constrained by the present data (i.e., involving the least number of unknowns).

The preferred model. The modification made to the simplest model described in the preceding paragraphs is that the distribution of OH groups is no longer assumed to be always random, although the random distribution is assumed at equilibrium. That is, we ignore the nonideal mixing behavior and the preferred association or avoidance of H_2O, OH, and anhydrous O, which are implied by a regular solution fit to the equilibrium speciation data (Silver and Stolper, 1989; Stolper, 1989; Silver et al., 1990; Zhang et al., 1991). Homogeneous reaction in the condensed state is in general influenced by both diffusion and reaction (Rice, 1985). Diffusion tries to maintain the concentration of OH pairs to that at random distribution, but reaction produces or consumes OH pairs, and hence disturbs the random distribution of OH groups. To describe the rate of a reaction in which diffusion is not infinitely fast, it is necessary to account for the role of reaction in disturbing the distribution of species and of microscopic diffusion of OH groups in rehomogenizing the distribution after the disturbance.

The coupled diffusion-reaction problem is complicated. Although there have been many efforts in the chemical literature to deal with this problem, none is entirely satisfactory (Rice, 1985). In our case, it is impossible to consider the details of diffusion because the initial distribution of OH groups is not known. Therefore, the following relatively simple approach is adopted. The forward elementary reaction at the microscopic level is assumed to be $H_2O + O \rightarrow$ pair (rate constant k_f) and the backward reaction is pair $\rightarrow H_2O + O$ (rate constant k_b'), where "pair" means an OH pair. Ignoring the different subspecies of OH and O, the reaction law can be written as

$$\frac{d[H_2O]}{dt} = -k_f[H_2O][O] + k_b'[pair] \quad (9)$$

$$\frac{d[pair]}{dt} = k_f[H_2O][O] - k_b'[pair] + \text{diffusive terms.} \quad (10)$$

The diffusive terms can include both positive and negative contributions, bringing OH singletons together to form pairs or splitting apart the OH pairs already present. If the initial distribution of OH groups does not affect the randomization, an expression of the diffusive term can be derived as follows (Appendix 2; G. R. Gavalas, personal communication):

$$\text{diffusive terms:} \quad \frac{d[pair]}{dt} = k[OH_s]^2 - k'[pair] \quad (11)$$

where $[OH_s]$ means the concentration of OH singletons. The first term on the right side indicates that the rate of bringing OH groups together to form pairs is proportional to the square of the concentration of OH singletons (where k is related to the diffusivity of OH groups), whereas the second term indicates that every pair has a finite probability of splitting. The two parameters (k and k') in Equation 11 are related by

$$k[OH_s]_r^2 = k'[pair]_r \quad (12)$$

where the subscript "r" stands for random distribution (note that the subscript "r" in τ_r stands for relaxation). Substituting Equation 11 into Equation 10 yields

$$\frac{d[pair]}{dt} = k_f[H_2O][O] - k_b'[pair] + k[OH_s]^2 - k'[pair]. \quad (13)$$

The concentrations of OH singletons and pairs at random distribution are estimated as follows. Let the number of O neighbors of each OH group be Z (assumed to be 12 as in closest packing). The probability that a nearest neighbor is not an OH group is $1 - [OH]$. Therefore the probability that all Z neighbors are non-OH is $(1 - [OH])^Z$. Hence

$$[OH_s]_r = [OH](1 - [OH])^Z. \quad (14)$$

All the other OH groups have at least one OH neighbor and thus are capable of converting to H_2O. Most of these clusters are pairs, some are triplets, etc. The concentration of OH pairs, [pair], is approximated by

$$[pair] \approx ([OH] - [OH_s])/2 \quad (15)$$

where the factor ½ is due to the fact that a pair requires two OH groups. Triplets, etc. are included in this definition of [pair]. This causes some error in the model because two triplets that are far away from each other can at most form two H_2O molecules, but by this definition they would be able to form three H_2O molecules. Combining Equations 14 and 15 yields

$$[pair]_r = \frac{[OH] - [OH_s]_r}{2} = \frac{[OH]}{2}[1 - (1 - [OH])^Z]. \quad (16)$$

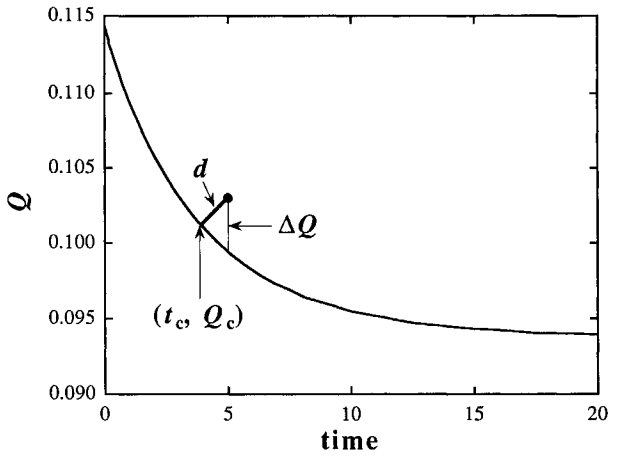

Fig. 6. Illustration of d used in the fitting procedure, which is the smallest distance (normalized to error in t and Q of each point) between the point and the curve, while ΔQ is the difference in Q between the point and the curve at the same time. In this plot, the length of error bar in time and that in Q are identical. In our minimization procedure, we minimized Σd_i^2 instead of $\Sigma (\Delta Q_i)^2$.

At low OH concentration, the right side of Equation 16 becomes approximately $Z[OH]^2/2$, similar to Equation 14.17 in Denbigh (1981) and to Equation 8. Since at equilibrium the net reaction rate must be zero (i.e., d[pair]/dt = 0 in Eq. 13) and the distribution is assumed to be random (i.e., [pair] = [pair]$_r$), the parameter k'_b can be found from Equations 13 and 16 to be

$$k'_b = k_f \frac{[H_2O]_e[O]_e}{[pair]_e} = k_f \frac{[H_2O]_e[O]_e}{\frac{[OH]_e}{2}[1 - (1 - [OH]_e)^Z]} \quad (17)$$

where the subscript "e" refers to the equilibrium concentration.

Equations 9 and 13 describe our model for the reaction, with k' given by Equation 12 and k'_b given by Equation 17. Since K (and hence the equilibrium species concentrations) and initial species concentrations are known, three parameters (unknowns) are used to fit experimental data, k_f, k, and $[pair]_0$, the initial concentration of OH pairs.

Alternative models. Before going into the modeling results based on the equations developed in previous paragraphs, we will first describe alternative models. One model that we considered takes into account the presence of both AlOH and SiOH as subspecies for OH groups (Zhang et al., 1990). There are four unknowns involved in using two subspecies of OH groups. However, even with one more fitting parameter (i.e., four unknowns in this model compared to three unknowns in our preferred model), this model does not generate significantly better fits to the experimental data than the preferred model. Other models that we tried invoked other intermediate and unmeasurable species. These models are in general complicated and upon preliminary examination did not yield better fits to our experimental data. Another area for improvement would be to consider the effects of nonideal mixing behavior. However, this would complicate the fitting even more. Based on all these exercises, we conclude that the reaction is complicated, and that a complete and accurate description of the reaction mechanism is not yet possible. Consequently, our more modest goal based on the present data set has been to fit the experimental data as well as possible in the context of a relatively simple model and thereby to gain insight into some of the major factors affecting the kinetics of the interconversion of H_2O molecules and OH groups.

Modeling results. This section presents modeling results based on Equations 9 and 13. Experimental Q vs. t data for each sample were fit by a least-squares procedure that yields values for the three adjustable parameters in the model, k_f, k, and $[pair]_0$. Since errors in experiment duration for higher T samples are sometimes significant, the sum of the squares of the distances of all points to the calculated curve was minimized in the fitting instead of the conventional χ^2. That is, Σd_i^2 was minimized, where d_i is the distance of point i to the calculated curve normalized to the error of the data and is defined as

$$d_i = \left(\frac{t_d - t_c}{\sigma_t}\right)_i^2 + \left(\frac{Q_d - Q_c}{\sigma_Q}\right)_i^2 \quad (18)$$

where t_d and t_c are experimental and calculated time, Q_d and Q_c are the experimental and calculated Q, and σ_t and σ_Q are the errors associated with the time and concentration. The parameters t_c and Q_c are chosen on the calculated curve such that d_i is the smallest distance from point i to the curve (Fig. 6) using a one-dimensional minimization routine. The Levenberg-Marquardt method (Press et al., 1989) was used to minimize Σd_i^2. Given initial estimates of the three unknowns (k_f, k, and $[pair]_0$), the time evolution of $[H_2O]$ and [OH] (and hence Q) was calculated. Given this calculated curve and the experimental data points, d_i, Σd_i^2, and the derivatives of d_i with respect to the three unknowns were calculated. New estimates of the three unknowns were then found with the Levenberg-Marquardt method. This procedure was repeated until Σd_i^2 was minimized.

Two numerical problems were encountered in fitting the experimental data. One problem arises because there are only five to ten experimental points in each Q vs. t curve through which a three-parameter curve is fit. Consequently, the parameters are sometimes not well-constrained (for a detailed example of how well a parameter is constrained, see the contour method of Feng and Savin, 1993). For example, the best fit k_f for sample F-D3B at 500 °C (five data points) is 0.8 ± 27.6 min^{-1}. In such cases, some parameters were estimated based on information from related experiments in which the parameters were better constrained and the data were fitted again. A second numerical problem, also the result of insufficient data points, is the occurrence of unwanted oscillations in the fit, which is analogous to what can happen when data are fit with a polynomial of too high an order. Each fit was checked visually for such unwanted oscillations, and this problem was encountered in only one case (C-D1C

TABLE 3. Fitting results

Sample	Total water (wt%)	K	k_f (min^{-1})	k (min^{-1})	Ratio	$\sqrt{\Sigma d_i^2/(n-1)}$
			600 °C			
G-D4	0.8	0.150*	~1	6.1 ± 1.6	2.4 ± 0.6	0.79
E-D2A	0.86	0.148	~1	2.3 ± 1.0	1.17 ± 0.04	0.64
C-D1C	1.0	0.139	~1	~13.1	~1.22	0.67
			550 °C			
A-D2C	2.3	0.103	~0.86	14 ± 20	1.09 ± 0.14	1.57
B-D1B-1	1.3	0.1125	~0.85	~8.5	1.10 ± 0.02	0.38
B-D1B-2&4	1.3	0.1125	0.85 ± 0.29	8.5 ± 9.1	1**	0.93
B-D1B-3	1.3	0.1125	~0.85	~8.5	1.12 ± 0.07	1.69
B-D6A	1.4	0.108	~0.86	2.6 ± 5.3	1.05 ± 0.05	1.40
F-D4B (pt.1)	0.80	0.121	0.95 ± 0.78	2.6 ± 1.2	1.27 ± 0.08	0.95
F-D4B (pt.2)	0.76	0.122	~0.95	~2.6	1.24 ± 0.03	0.99
			500 °C†			
B-D1B	1.3	0.0920	0.080 ± 0.025	0.135 ± 0.202	1.06 ± 0.03	0.93
B-D5A	0.5	0.1005*	0.143 ± 0.111	0.031 ± 0.009	0.63 ± 0.04	1.00
D-D1 (pt.1)	0.9	0.0960	0.149 ± 0.066	0.305 ± 0.030	0.85 ± 0.04	0.35
D-D1 (pt.2)	1.0	0.0945	0.101 ± 0.029	0.320 ± 0.042	0.94 ± 0.05	0.32
H-D1B (pt.1)	0.78	0.0976*	~0.1	0.039 ± 0.013	1.57 ± 0.05	1.51
H-D1B (pt.2)	0.72	0.0983*	~0.1	0.033 ± 0.009	1.51 ± 0.03	0.98
F-D3B	0.8	0.0973*	~0.1	0.088 ± 0.069	0.94 ± 0.04	1.74
G-D1A	0.77	0.0978*	~0.1	0.095 ± 0.049	1.27 ± 0.06	1.76
E-D1A	0.9	0.0964*	0.173 ± 0.076	0.181 ± 0.017	0.87 ± 0.02	0.33
C-D2A	1.1	0.0930	~0.1	0.445 ± 0.089	1.21 ± 0.03	0.64
			482 °C			
H-D2A (pt.1)	0.80	0.0904*	~0.139	0.0107 ± 0.0015	1.41 ± 0.02	0.82
H-D2A (pt.5)	0.88	0.0896*	~0.139	0.0178 ± 0.0028	1.47 ± 0.03	1.18
H-D2A (pt.7)	0.77	0.0906*	~0.139	0.0086 ± 0.0036	1.41 ± 0.05	2.03
E-D3	0.87	0.0892	0.139 ± 0.082	0.072 ± 0.010	0.81 ± 0.03	1.56
			400 °C			
A-D2C	2.3	0.0512*	0.188 ± 0.049	0.273 ± 0.027	0.78 ± 0.02	0.30
A-D2D	2.6	0.0500*	0.135 ± 0.059	0.193 ± 0.035	0.82 ± 0.03	0.75
			Albitic glass			
500 °C	1.0	~0.235	~0.5	0.122 ± 0.025	0.44 ± 0.054	2.29
600 °C	1.0	0.302	0.56 ± 0.36	2.1 ± 15.0	0.95 ± 0.13	0.52
550 °C	1.0	0.248	0.24 ± 0.06	0.79 ± 0.80	1**	1.12

Note: see Table 1 for sample numbers. Ratio = $[pair]_0/[pair]_{0,r}$. Errors are 2σ errors. Sometimes the 1σ error for a parameter is greater than the value itself, indicating that the parameter is not constrained by the experimental data. In these cases, the parameter is estimated from experiments involving similar samples at the same temperature, and the value is prefixed by ~. Other parameters for the sample are obtained by fitting. However, the given errors for these are unrealistic and smaller than the real errors since one parameter was arbitrarily fixed.

* Equilibrium is not reached in the experiment, K is calculated from Zhang et al. (1991).

** The ratio $[pair]_0/[pair]_{0,r}$ is assumed to be 1 because the starting material was preequilibrated.

† Weighted average of k_f of all samples at 500 °C = 0.099 ± 0.059 min^{-1}.

at 600 °C). In this case, the best fit solution was discarded in favor of a solution found by trial-and-error that still fits the data well without unwanted oscillations.

Excellent fits were obtained for the time evolution of speciation of most samples. All fits are reported in Table 3 and some are shown in Figures 1 and 2. Of all fits, the fit in Figure 2A for an albitic glass shows the most systematic departure from the data, perhaps because the sample was prepared at a high pressure. The ratio of the initial OH-pair concentration to that at random distribution ($[pair]_0/[pair]_{0,r}$) is in all cases on the order of 1 (0.44–1.57, except for G-D4 at 600 °C, which has a ratio of 2.4 ± 0.6), suggesting that the initial departure from random distribution is not very large and that the value of $[pair]_0$ is meaningful. Another indication of the significance of $[pair]_0$ and the internal consistency of this model comes from the modeling results of experiments at 550 °C involving two rhyolitic glasses (B-D1B-2 and B-D1B-4) and the albite glass (ABC-26). Prior to the 550 °C experiments, B-D1B-2 and B-D1B-4 were preequilibrated at 500 °C and ABC-26 was preequilibrated at 600 °C. The initial concentration of OH pairs is expected to be very close to that of a random distribution (i.e., $[pair]_0/[pair]_{0,r} = 1$) for these samples. And indeed, the experimental results can be fit well by using $[pair]_0/[pair]_{0,r} = 1$, and the best fit values are nearly identical to 1 (1.00 ± 0.06 for combined B-D1B2 and B-D1B4; 0.90 ± 0.07 for albite). Fitting results indicate that within error, k_f is almost independent of total water content (see five fitting results for k_f at 500 °C and two fitting results at 550 °C in Table 3). On the other hand, k is strongly dependent on water content. This is not well understood but could be related to structural variations such as depolymerization accompanying the formation of OH groups.

Despite the overall success of the model at reproducing the experimental results, there are still some problems. One is the large uncertainties of k_f and k, the parameters needed to apply the experimental results to natural sys-

TABLE 4. Apparent equilibrium temperature and cooling rate of obsidian glasses

Sample	Water (wt%)	T_{ae} (°C)	q at T_{ae} (°C/s)	Locality
A-D2C	2.36	510	3.8	1
B-D1B	1.31	540	1.0	1
B-D5A	0.50	700	2.0	1
B-D6A	1.43	540	1.5	1
D-D1 (pt.1)	0.90	640	5.2	1
D-D1 (pt.2)	0.95	630	5.5	1
H-D1B (pt.1)	0.77	430	0.0005	2
H-D1B (pt.2)	0.70	430	0.0003	2
H-D2A (pt.1)	0.80	425	0.0004	2
H-D2A (pt.5)	0.88	420	0.0006	2
H-D2A (pt.7)	0.77	435	0.0006	2
F-D3B	0.80	550	0.13	3
F-D4B	0.77	545	0.09	3
G-D1A	0.77	475	0.0025	4
G-D4	0.79	460	0.005	4
E-D1A	0.87	620	2.4	5
E-D2A	0.85	620	2.2	5
E-D3	0.85	620	2.2	5
C-D1C	1.09	450	0.007	6
C-D2A	1.08	450	0.007	6

Note: see Table 1 for sample numbers. Locality: 1 = Mono Craters (site bb, Sieh and Bursik, 1986; Newman et al., 1988); 2 and 3 = Mono Craters (exact site unknown); 4 = unknown location; 5 = Mono Craters (site K); 6 = Mono Craters (site L).

tems. Although there are general trends in k_r and k with temperature and water content, the large errors make it impossible to quantify them with any certainty. Consequently, although it is possible to estimate the quench rate from speciation data using Equation 6, we are not yet in a position to quantitatively predict how speciation would change given a complicated thermal history. The second problem is that a few fits are not very good when viewed visually, although $\sqrt{\Sigma d_i^2/(n-1)}$ is not large. The third is that the parameter $[pair]_0$ is not very robust. For example, three similar samples were heated at different temperatures, E-D2A at 600 °C, E-D1A at 500 °C, and E-D3 at 482 °C. Ideally, the $[pair]_0/[pair]_{0,r}$ ratios for all three samples should be identical. However, the fits give 1.17 ± 0.04, 0.87 ± 0.02, and 0.81 ± 0.03, respectively. Although all values are near unity, the differences are outside the error of the fitting parameters.

Undoubtedly, some of the problems described in the last paragraph stem from oversimplifications implicit in Equations 9 and 13. However, in spite of these problems, the overall success of this model is encouraging, and the model appears to be a good first approximation considering the complexity of the problem. Moreover, this model has some interesting implications. For example, Zhang et al. (1991) have shown that diffusion of water in silicate melts and glasses involves the interconversion reaction between the species, and that the diffusivity of molecular H_2O is so much greater than that of OH groups that the contribution of OH diffusion to total water diffusion can be ignored. The model adopted here requires the consideration of slow OH diffusion (see Appendix 2 for an estimate of D_{OH} that confirms $D_{OH} \ll D_{H_2O}$) to form OH pairs available for reaction. Thus, the diffusion and reaction processes are intimately coupled.

Thermal history of natural obsidian glasses

Our data can be applied to natural obsidian glasses to infer their thermal histories. If the reaction between H_2O molecules and OH groups were simple, only the cooling rate at the T_{ae} (i.e., dT/dt at $T = T_{ae}$) could be inferred (e.g., Ganguly, 1982; Newman et al., 1993; Zhang, 1994). However, the reaction mechanism is relatively complex. Even though the complexity of the reaction makes it more difficult to characterize, the complexity would allow, in principle, the inference of whether cooling was monotonic. This inference would be potentially valuable in the study of volcanic glasses, which in the processes of eruption, emplacement, and burial have many opportunities for exposure to multiple heating and cooling events.

Simple cooling rates. The apparent equilibrium temperature of each natural obsidian glass can be readily determined from the measured hydrous speciation (Zhang et al., 1991). If there were no loss or addition of water from the glasses after quenching from high temperature, then the quench rate at $T = T_{ae}$ can be estimated from T_{ae} using Equation 6 by ignoring the complex reaction mechanism and assuming monotonic cooling. Whether or not there was significant hydration or dehydration of the samples has to be evaluated case by case. We tentatively suggest that hydration and dehydration after the glasses were quenched are not significant based on the freshness of the glasses (frosted surfaces are polished away before the analyses) and the homogeneity of the samples in terms of H_2O and OH contents. Table 4 reports values of T_{ae} and estimated quench rates based on Equation 6 for the natural volcanic glasses used as starting materials in this study. The isothermal experimental data in Figure 3 were also used to estimate the quench rates for the natural samples; the results roughly agree with those in Table 4. The cooling rates of other volcanic glasses were also estimated, using Equation 6 as the basis for interpolation and extrapolation. Newman et al. (1988) measured the speciation of water in obsidian glasses (pyroclasts, surge deposits, and block-and-ash flow) from the Mono Craters. We also collected more glasses from site "bb" and measured the speciation. The cooling rates for these natural glasses vary by four orders of magnitude, from 0.0003 to 5.5 °C/s. Even though errors in estimating cooling rates are large (a factor of four), these differences in the cooling rates of hydrous obsidian glasses are so large that they are readily distinguishable. In Figure 4, all pyroclastic glasses from site bb follow the same trend as experimental glasses quenched by compressed air flow (slow quench, Ihinger, 1991), as expected. The E glasses (Table 4) also have quench rates similar to the air-quench experiments. Other samples have significantly lower cooling rates: ~0.1 °C/s for glass F (which is a large piece of glass), surge deposits, and a large piece from Bed 8 (Newman et al., 1988); ~0.01 °C/s for glasses from block-and-ash flow (Newman et al., 1988); ~0.005 °C/s for the C and G glasses; and ~0.0005 °C/s (40 °C/d) for the H glasses.

Anderson et al. (1989) reported the speciation of water in glass inclusions in quartz phenocrysts from two strati-

graphic levels in the Bishop Tuff. Based on the good to excellent data indicated in Table 2 of Anderson et al. (1989), cooling rates range from 0.01 to 0.2 °C/s for glass inclusions in quartz phenocrysts in the plinian deposits, and from 3×10^{-5} to 3×10^{-4} °C/s for glass inclusions in quartz phenocrysts in the Mono lobe ash flow deposits. The slower cooling rates inferred for the latter inclusions are consistent with the conclusions of Stolper (1989).

Complex cooling history. The cooling rates inferred above based on the observed speciation of obsidians do not, however, tell the whole story. In the context of this modeling, the details of the experimentally determined Q vs. t trends provide additional information. For example, when sample F-D4B is heated at 550 °C (Fig. 1B), H-D1B at 500 °C, and H-D2A.7 at 482 °C (Fig. 1E), the observed Q first decreases and then increases. In contrast, when the synthetic albitic glass quenched from 20 kbar and 1400 °C in a piston cylinder apparatus (Silver and Stolper, 1989) is heated at 500 °C, the observed Q first increases and then decreases (Fig. 2A). These observations are fairly well fit by the diffusion-reaction model and can be understood in the following way. For a monotonically cooled sample, the distribution rerandomizes rapidly as OH pairs convert to H_2O molecules if T_0 is much greater than T_{ae}. On cooling, as T approaches T_{ae}, OH pairs are continuously converted into H_2O molecules (because the reaction pair = H_2O + O tries to reach equilibrium at low temperatures), but there is insufficient time to rerandomize the new, OH-poorer distribution of OH groups. Consequently, in samples cooled monotonically from well above T_{ae}, the frozen-in distribution is expected to be deficient in OH pairs, as observed in the albitic glass starting materials. Therefore, even though the albitic glass initiallly had an excess of OH groups relative to the equilibrium value at 500 °C (i.e., $Q > K$), when the sample was subsequently heated at 500 °C, H_2O molecules initially convert into OH pairs because of the underabundance of OH pairs with respect to the reaction H_2O + O = pair, leading to an initial increase in Q away from K. After the concentration of OH pairs is brought to a high concentration by consuming H_2O and by OH diffusion, the reaction becomes "normal" and Q decreases toward K.

An underabundance of OH pairs is expected if the sample is prepared by cooling from a high temperature, as described in the preceding paragraph. Some of the natural glasses (such as the A, B-D5, and D samples) appear to have this kind of distribution even though they do not show the nonmonotonic behavior of the albitic glass (Table 3 and Fig. 1). All of these glasses have $[pair]_0/[pair]_{0,r} < 1$ (as well as the highest inferred quench rates). However, some natural samples seem to have an overabundance of OH pairs relative to a random distribution. These samples have lower inferred quench rates, and there seems to be an inverse correlation between the parameter $[pair]_0/[pair]_{0,r}$ and the inferred cooling rate. When these samples are heated, the overabundance of OH pairs makes the backward reaction more prominent, and hence H_2O concentration increases and Q decreases. If the overabundance of OH pairs is great enough, Q can still decrease even if initial Q is smaller than or equal to K, and this leads to the minimum observed in some Q vs. t trends (F-D4B in Fig. 1B and H-D2A in Fig. 1E). As the overabundant OH pairs are consumed by reaction and diffusion, the reaction gradually resumes its normal course and Q increases toward equilibrium.

The inferred overabundance of OH pairs in these natural samples was unanticipated. Since the overabundance of OH pairs is defined by $[pair]_0/[pair]_{0,r} > 1$, the OH pairs are overabundant when compared to the total OH content, and an underabundance of H_2O molecules owing to low-temperature dehydration of the glass cannot be responsible for it. The simplest explanation for the inferred overabundance of OH pairs is that these obsidians underwent a complex thermal history. An example of a thermal history that could explain these data would be as follows: the sample was first cooled relatively slowly such that it had a T_{ae} lower than its present-day T_{ae}, then rapidly brought to a higher temperature to generate excess OH pairs, and then quenched rapidly enough to preserve the overabundance of OH pairs. This type of thermal history is not as ad hoc or implausible as it may at first appear. Newman et al. (1988) noted that the existence and preservation of these water-rich obsidian clasts is paradoxical, since if they were erupted at magmatic temperatures, they would surely have vesiculated and converted to pumice on eruption. Newman et al. (1988) proposed that these obsidians formed as glass selvages lining volcanic conduits or dikes that were subsequently caught up in the explosive eruption of the Mono Craters. In this context, the inferred thermal history is precisely what one expects: slowly cooled glasses formed at the conduit margin but were transiently reheated for seconds to minutes when they were caught up in the 750–850 °C eruption that brought them to the surface, then they rapidly quenched on eruption.

For samples that had a transient heating event, the T_{ae} of the glass before the transient heating event would have been lower than that calculated above using Equation 6 and reported in Table 4. Some H_2O molecules would have been converted to OH pairs during the transient heating, and hence H_2O concentration before the transient heating was greater than that measured in the natural sample. Although the presence of such a transient heating event may be inferred from the experimental data, in the future a better understanding and quantification of the reaction mechanism will be necessary to constrain further thermal history of natural glasses.

Although our inference of the thermal histories of obsidian glasses from the Mono Craters is nonunique and needs to be confirmed, the implications of the measured species concentrations and the observed Q vs. t trends are important. The very existence of water-rich obsidians in these deposits is enigmatic, and the complex, at least two-stage thermal histories inferred for some of these samples are consistent with the hypothesis of Newman et al. (1988) that these samples are fragments of quenched, glassy dikes or conduit rinds that were caught up and transiently reheated in an eruption. These data on natural

obsidians reveal a surprising richness in the details of the speciation of water in volcanic glasses and show how, at least in principle, quantitative constraints on their thermal histories can be extracted by application of kinetic models.

Conclusions

Experiments have been conducted to examine the kinetics of the reaction $H_2O + O \rightleftharpoons 2OH$ at constant temperature in the range of 400–600 °C. Experimental data indicate that (1) the reaction rate increases with temperature and water content, and (2) the reaction mechanism is complex and may involve diffusion and/or intermediate species. When the isothermal experimental results of this study are compared with the results of previous experiments that examined the dependence of speciation on quench rate, the two sets of data are compatible and complementary. An analysis of the quench rates vs. speciation data yields a relation between the quench rate, the apparent equilibrium temperature of the quenched species, and the water content. Based on both the isothermal kinetic data and the quench-rate speciation data, we conclude that speciation data of rapid-quench cold-seal experiments and 1-atm experiments from this lab are not affected by reaction during quench as long as total water content is <2.0% at 600 °C, 3.2% at 550 °C, and 5.5% at 500 °C. However, speciation in glasses with ≥0.8% total water content quenched from 850 °C reflects a lower apparent equilibrium temperature, which decreases with increasing water content and decreasing cooling rate.

In detail, the reaction mechanism is inferred to be complex based on the variation of speciation with time in isothermal experiments. Diffusion of OH groups may play an important role and there may be subspecies or intermediate species involved in the reaction. We have modeled the forward and backward reactions as follows: the forward reaction is simple but the backward reaction requires two steps: first, two OH groups come together to form a pair, then the pair reacts to form an H_2O molecule and an anhydrous O. This model accounts for the data fairly well, though there are still problems. More detailed data will be needed to refine or revise our understanding of the reaction mechanism.

The above results have been used to estimate the cooling history of volcanic glasses. The estimated cooling rates for natural rhyolitic glasses vary by four orders of magnitude, ranging from 0.0003 to 5.5 °C/s. Glass inclusions may have even slower cooling rates. Based on our model results, some glasses seem to have had complex thermal histories involving slow cooling, then rapid transient heating, and finally even more rapid quench, consistent with previous inferences.

Acknowledgments

Discussions with G.R. Gavalas (of California Institute of Technology), A.C. Lasaga, and S. Newman have been most helpful. Comments by D.B. Dingwell, E.J. Essene, R.A. Lange, H.N. Pollack, E.B. Watson, B.H. Wilkinson, and an anonymous reviewer are appreciated. Y.Z. thanks J.G. Blank and P.F. Dobson for their help in collecting some of the samples from the "bb" site used in this study, and R. Belcher for some FTIR analyses. This work was supported by NSF grants EAR-8916707, EAR-9219899, EAR-9304161, and EAR-9315918 and DOE grant DE-FG03-85ER13445. Division of Geological and Planetary Sciences Contribution no. 5386.

References cited

Anderson, A.T., Jr., Newman, S., Williams, S.N., Druitt, T.H., Skirius, C., and Stolper, E. (1989) H_2O, CO_2, Cl and gas in Plinian and ash-flow Bishop rhyolite. Geology, 17, 221–225.

Bartholomew, R.F. (1982) Water in glass. Treatise of Materials Science Technology, 22, 75–127.

Bartholomew, R.F., and Schreurs, J.W.H. (1980) Wide-line NMR study of the protons in hydrosilicate glasses of different water content. Journal of Non-Crystalline Solids, 38/39, 679–684.

Bartholomew, R.F., Butler, B.L., Hoover, H.L., and Wu, C.K. (1980) Infrared spectra of a water-containing glass. Journal of the American Ceramic Society, 63, 481–485.

Burnham, C.W. (1975) Water and magmas: A mixing model. Geochimica et Cosmochimica Acta, 39, 1077–1084.

Denbigh, K. (1981) The principles of chemical equilibrium, 494 p. Cambridge University Press, Cambridge, U.K.

Dingwell, D.B., and Webb, S.L. (1990) Relaxation in silicate melts. European Journal of Mineralogy, 2, 427–449.

Dobson, P.F., Epstein, S., and Stolper, E.M. (1989) Hydrogen isotope fractionation between coexisting vapor and silicate glasses and melts at low pressure. Geochimica et Cosmochimica Acta, 53, 2723–2730.

Eckert, H., Yesinowski, J.P., Stolper, E.M., Stanton, T.R., and Holloway, J. (1987) The state of water in rhyolitic glasses: A deuterium NMR study. Journal of Non-Crystalline Solids, 93, 93–114.

Eckert, H., Yesinowski, J.P., Silver, L.A., and Stolper, E.M. (1988) Water in silicate glasses: Quantitation and structural studies by ^1H solid echo and MAS-NMR methods. Journal of Physical Chemistry, 92, 2055–2064.

Eckert, H., Yesinowski, J.P., and Stolper, E.M. (1989) Quantitative NMR studies of water in silicate glasses. Solid State Ionics, 32/33, 298–313.

Feng, X., and Savin, S.M. (1993) Oxygen isotope studies of zeolites: Stiblite, analcime, heulandite and clinoptilolite: II. Kinetics and mechanism of isotopic exchange between zeolites and water vapor. Geochimica et Cosmochimica Acta, 57, 4219–4238.

Ganguly, J. (1982) Mg-Fe order-disorder in ferromagnesian silicates: II. Thermodynamics, kinetics and geological applications. In S.K. Saxena, Ed., Advances in physical geochemistry, vol. 2, p. 58–99. Springer-Verlag, New York.

Ihinger, P.D. (1991) An experimental study of the interaction of water with granitic melt. Ph.D. thesis, California Institute of Technology, Pasadena, California.

Keppler, H., and Bagdassarov, N.S. (1993) High-temperature FTIR spectra of H_2O in rhyolite melt to 1300 °C. American Mineralogist, 78, 1324–1327.

Kohn, S.C., Dupree, R., and Smith, M.E. (1989a) A multinuclear magnetic resonance study of the structure of hydrous albite glasses. Geochimica et Cosmochimica Acta, 53, 2925–2935.

——— (1989b) Proton environments and hydrogen-bonding in hydrous silicate glasses from proton NMR. Nature, 337, 539–541.

Lasaga, A.C. (1981) Rate laws and chemical reactions. In Mineralogical Society of America Reviews in Mineralogy, 8, 1–68.

McMillan, P.F. (1989) Raman spectroscopy in mineralogy and geochemistry. Annual Review of Earth and Planetary Sciences, 17, 225–283.

McMillan, P.F., and Remmele, R.L., Jr. (1986) Hydroxyl sites in SiO_2 glass: A note on infrared and Raman spectra. American Mineralogist, 71, 772–778.

Mysen, B.O. (1992) Peralkalinity, Al↔Si substitution, and solubility mechanisms of H_2O in aluminosilicate melts. Journal of Petrology, 33, 347–375.

Mysen, B.O., and Virgo, D. (1986a) Volatiles in silicate melts at high pressure and temperature: I. Interaction between OH groups and Si^{4+}, Al^{3+}, Ca^{2+}, Na^+ and H^+. Chemical Geology, 57, 303–331.

——— (1986b) Volatiles in silicate melts at high pressure and temperature: II. Water in melts along the join $NaAlO_2$-SiO_2 and a comparison

of solubility mechanisms of water and fluorine. Chemical Geology, 57, 333–358.
Newman, S., Stolper, E.M., and Epstein, S. (1986) Measurement of water in rhyolitic glasses: Calibration of an infrared spectroscopic technique. American Mineralogist, 71, 1527–1541.
Newman, S., Epstein, S., and Stolper, E. (1988) Water, carbon dioxide, and hydrogen isotopes in glasses from the ca. 1340 A.D. eruption of the Mono Craters, California: Constraints on degassing phenomena and initial volatile content. Journal of Volcanology and Geothermal Research, 35, 75–96.
Newman, S., Blouke, K., Bashir, N., Ihinger, P., and Stolper, E. (1993) Cooling of rhyolitic vocanics—evidence from melt inclusions. Geological Society of America Abstracts with Programs, 25, A-43.
Press, W.H., Flannery, B.P., Teukolsky, S.A., and Vetterling, W.T. (1989) Numerical recipes, 702 p. Cambridge University Press, Cambridge, U.K.
Rice, S.A. (1985) Diffusion-limited reactions, 404 p. Elsevier, Amsterdam.
Scholze, H. (1959) Der Einbau des Wassers in Gläsern: IV. Der Einfluß der Temperatur. Glastechnische Berichte, 32, 314–320.
Shaw, H.R. (1972) Viscosities of magmatic silicate liquids: An empirical method of prediction. American Journal of Science, 272, 870–893.
Sieh, K., and Bursik, M. (1986) Most recent eruption of the Mono Craters, eastern central California. Journal of Geophysical Research, 91, 12539–12571.
Silver, L.A., and Stolper, E.M. (1989) Water in albitic glasses. Journal of Petrology, 30, 667–709.
Silver, L.A., Ihinger, P.D., and Stolper, E.M. (1990) The influence of bulk composition on the speciation of water in silicate glasses. Contributions to Mineralogy and Petrology, 104, 142–162.
Skirius, C.M., Peterson, J.W., and Anderson, A.T., Jr. (1990) Homogenizing rhyolitic glass inclusions from the Bishop Tuff. American Mineralogist, 75, 1381–1398.
Stolper, E.M. (1982a) Water in silicate glasses: An infrared spectroscopic study. Contributions to Mineralogy and Petrology, 81, 1–17.
——— (1982b) The speciation of water in silicate melts. Geochimica et Cosmochimica Acta, 46, 2609–2620.
——— (1989) Temperature dependence of the speciation of water in rhyolitic melts and glasses. American Mineralogist, 74, 1247–1257.
Sykes, D., and Kubicki, J.D. (1993) A model for H_2O solubility mechanisms in albite melts from infrared spectroscopy and molecular orbital calculations. Geochimica et Cosmochimica Acta, 57, 1039–1052.
Taylor, B.E. (1986) Magmatic volatiles: Isotopic variation of C, H, and S. In Mineralogical Society of America Reviews in Mineralogy, 16, 185–225.
Zhang, Y. (1994) Reaction kinetics, geospeedometry, and relaxation theory. Earth and Planetary Science Letters, 122, 373–391.
Zhang, Y., and Stolper, E.M. (1991) Water diffusion in basaltic melts. Nature, 351, 306–309.
Zhang, Y., Stolper, E.M., and Ihinger, P.D. (1990) Reaction kinetics of $H_2O + O = 2OH$ and its equilibrium, revisited. V.M. Goldschmidt Conference 1990, 94.
Zhang, Y., Stolper, E.M., and Wasserburg, G.J. (1991) Diffusion of water in rhyolitic glasses. Geochimica et Cosmochimica Acta, 55, 441–456.

Manuscript received April 7, 1994
Manuscript accepted January 23, 1995

Appendix 1. More discussion on quench effects

We have concluded that the speciation recorded by the quenched glasses reported in this study, Stolper (1989), and Zhang et al. (1991) reflects the speciation at experimental temperatures and is uninfluenced by changes occurring on quenching. This conclusion is based on (1) the convergence of Q from higher and lower initial values to a single value (Fig. 1); (2) the long time scale required for equilibration under these conditions relative to the quenching time scale of ~1 s; and (3) the systematic dependence of the converged values of K on the temperature of heat treatment (such as data shown in Fig. 5). An implicit assumption in the reasoning, however, is that there is no subreaction in Reaction 1 that is fast enough to relax during quench in all the experiments. For example, if a subreaction had a T^*_{ae} (to distinguish it from T_{ae}, the apparent equilibrium temperature of the overall reaction) of 280 °C at the quench rate, this subreaction would always quench to the 280 °C speciation for experimental temperatures >280 °C. The above discussions, though extensive, do not rule out this possibility. Indeed, infrared and NMR spectroscopic studies have shown that some relaxation phenomena involving H-bearing species (although not necessarily involving interconversions among H_2O molecules and OH groups) occur at both high and low temperatures (Scholze, 1959; Bartholomew and Schreurs, 1980; Eckert et al., 1987; Keppler and Bagdassarov, 1993).

To evaluate explicitly this possibility, a series of experiments was designed based on the following reasoning. Suppose that the apparent temperature for the subreaction for a quenching time scale of 1 s is 280 °C for a sample. If the sample is held at 250 °C for a duration that is hundreds of times longer than 1 s (e.g., using a typical high-activation energy of 250 kJ/mol, τ at 250 °C is 23 times the τ at 280 °C), reaction at 250 °C for this subreaction would change the speciation relative to the one frozen in at 280 °C on a 1 s quench from higher temperature, but this 250 °C speciation would itself be preserved in a 1 s quench. Thus, an effective test of the hypothesis that there is such a rapid, low-temperature relaxation mechanism that contaminated all of our speciation experiments would be to hold a sample at, e.g., 500 °C for a sufficient duration to reach an equilibrium distribution of species, and then to hold the sample at 450, 400, 350, 300, 250, and 200 °C each for several hundred seconds. If there were a low-temperature relaxation mechanism, and assuming the activation energy is ≤250 kJ/mol, there would be a detectable shift in the value of Q in the vicinity of T^*_{ae} for this relaxation mechanism from a constant value for samples quenched from $T > T^*_{ae}$ to a different, again roughly constant value for samples quenched from $T < T^*_{ae}$.

Therefore, the following experiments were carried out: Sample D-D1.2 (0.94% total water) was first equilibrated at 500 °C (Fig. 1D). It was then held at 450, 400, 350, 300, and 250 °C each for 5 min and at 200 °C for 10 min to see if there is any change in speciation. Appendix Figure 1 shows the variation of Q vs. cumulative time for this sample. There is only a slight and probably insignificant change (the difference in terms of ln Q is 0.026, just at the limit of uncertainties of 0.022) at 450 °C, suggesting that the apparent equilibrium temperature for a 1 s quench time scale is significantly higher than 450 °C, and that there is no subreaction that has a T^*_{ae} between 200 and 400 °C. Although this test did not go all the way down to room temperature, it is unlikely that there is a subreaction that would have a T^*_{ae} below 200 °C. The species concentrations have also been measured at liquid N_2 temperature for several samples (that for D-D1 is shown in Table 1). The peak heights are on average (1.2 ± 2.4) higher than measurements at room temperature, but the calculated Q does not change significantly (Appendix Fig. 1). These results confirm that there is no significant portion of the reaction that relaxes to a T^*_{ae} lower than the experimental temperature during quench.

Appendix 2. Diffusive contribution to concentration of pairs

This appendix derives an approximate expression for the diffusive contribution to d[pair]/dt (Eq. 11). Owing to the random

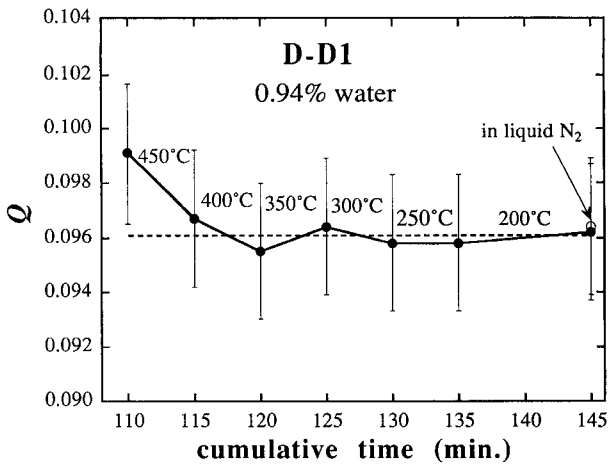

Appendix Fig. 1. Examination of whether or not there is a subreaction of Reaction 1 that has a T^*_{ae} below 450 °C. Sample D-D1 contains 0.94% total water. Error bar is 2.6% (relative) of the value. The first point shows that measurement after equilibrium is established at 500 °C (110 min). The sample was heated sequentially for 5 min each at 450, 400, 350, 300, and 250 °C, and for 10 min at 200 °C. The temperature for each time interval is marked. The point that follows the temperature is the speciation measured after heating at the temperature. Solid circles = measurement of quenched glass at room temperature, and open circle = in situ measurement in liquid N_2.

motion of OH groups, any OH pair has a finite probability to split, and this accounts for the second term on the right side of Equation 11. The first term can be derived as follows based on Rice (1985). Consider a singleton OH group in the structure. Other singleton OH groups approach it by random walking (diffusion). The variation of the OH concentration in the neighborhood of the singleton OH group is described by

$$\frac{\partial[OH_s]_{local}}{\partial t} = D_{OH}\frac{1}{r}\frac{\partial^2}{\partial r^2}(r[OH_s]_{local}) \quad (A1)$$

where r is the distance away from the OH group, $[OH_s]_{local}$ is the local concentration of singleton OH groups (as compared to the bulk or average concentration of OH singletons), and D_{OH} is the diffusivity of OH groups (which is much smaller than the diffusivity of molecular H_2O, Zhang et al., 1991). At steady state (i.e., when the initial distribution of OH groups does not play a significant role; we are forced to this simplification because we do not know the detailed initial distribution of pairs), the left side of the above equation (and hence the right side) is zero. That is,

$$D_{OH}\frac{1}{r}\frac{\partial^2}{\partial r^2}(r[OH_s]_{local}) = 0. \quad (A2)$$

The solution to the above equation is

$$[OH_s]_{local} = A + \frac{B}{r}. \quad (A3)$$

We need the boundary conditions to fix parameters A and B. At $r = a$, where a is the radius of the singleton OH group, there is no other OH group (otherwise the OH group is not a singleton). Hence $[OH_s]_{local,r=a} = 0$. The other boundary condition is that at $r = \infty$, the conentration of OH singletons is the same as the bulk (or average) concentration:

$$[OH_s]_{local,r=a} = [OH_s]_{bulk} = [OH_s]. \quad (A4)$$

Using the boundary conditions to find A and B in (A3), we have

$$[OH_s]_{local} = [OH_s]\left(1 - \frac{a}{r}\right). \quad (A5)$$

The total flux of OH to the OH singleton is

$$4\pi a^2 D_{OH} N_O \frac{\partial[OH_s]_{local}}{\partial r}\bigg|_{r=a} = 4\pi a D_{OH} N_O [OH_s] \quad (A6)$$

where N_O is the number of O atoms per unit volume. That is, the probability that one singleton OH will become paired is proportional to $[OH_s]$. For all OH singletons, the probability to form pairs is proportional to the number of OH singletons times the above flux. Therefore, the rate of forming OH pairs is proportional to the square of $[OH_s]$ (hence the first term in the right side of Eq. 11) with the proportionality k,

$$k = 0.0708 \times 2\pi a D_{OH} N_A \quad (A7)$$

where 0.0708 is the number of moles of O per cubic centimeters of glass, N_A is Avogadro's constant. D_{OH} can be estimated from k and is found to be $\sim 10^{-22}$ m²/s at 500 °C and ~1.0% total water. Therefore, D_{OH} is indeed many orders of magnitude lower than D_{H_2O} ($\sim 10^{-13}$ m²/s at 500 °C, Zhang et al., 1991), consistent with the conclusions of Zhang et al. (1991).